The Riemann problem for the Baer-Nunziato model of two-phase flows

Nikolai Andrianov and Gerald Warnecke*

October 29, 2002

Abstract

We consider the Riemann problem for the two-phase model, proposed by Baer and Nunziato in [*Int. J. of Multiphase Flows*, **12**, 861-889 (1986)]. It describes the flame spread and the deflagration-to-detonation transition (DDT) in gas-permeable, reactive granular materials. The model is given by the non-strictly hyperbolic, non-conservative system of partial differential equations. We investigate the structure of the Riemann problem and construct the exact solution for it. Furthermore, we define a weak solution for it and propose a number of test cases. Under certain conditions, the two-phase flow equations reduce to the Euler equations in the duct of variable cross section. Consequently, our construction of the exact solution applies also to this system.

1 Introduction

It is well known, that a large class of the two-phase flows is described with the non-conservative models, i.e., the corresponding system of governing equations cannot be written in divergence form, see e.g. [14]. Therefore, the notion of a weak solution cannot be defined in the usual manner, as it is done for the system of conservation laws. Another consequence of the non-conservativity of the models is that a large class of numerical methods, which have been successfully used for conservation laws, cannot be directly applied here. Note that the two-phase flow equations are basically quite similar to the (conservative) fluid dynamics equations and in fact reduce to them when the phase concentration does not change. Therefore, the usual practice is to take some numerical method for conservation laws and modify it in order to account for the non-conservation. Unfortunately, there are very few benchmark tests for validating and comparing

*IAN, Otto-von-Guericke Universität Magdeburg, PSF 4120, D-39016 Magdeburg, Germany. Email: {nikolai.andrianov | gerald.warnecke}@mathematik.uni-magdeburg.de

of the numerical methods for two-phase problems available. The present paper attempts to fill this gap to some extent.

One of the most established models in the theory of two-phase flows is the model, proposed in 1986 by Baer and Nunziato [2], see also Bdzil et. al. [3], Kapila et. al. [7], Embid and Baer [6]. In what follows, we will refer it to as the BN model. It describes the flame spread and the deflagration-to-detonation transition (DDT) in gas-permeable, reactive granular materials. Mathematically, the model is given by the set of the partial differential equations, which cannot be written in conservative form. Consequently, the above mentioned difficulties apply to this model, too.

Consider the Riemann problem for the BN model. The usual “direct” solution of the Riemann problem is achieved as follows: Given the end states $\mathbf{u}_L, \mathbf{u}_R$, one has to find the intermediate states. However, it is problematic to find it for the two-phase model, since the structure of the Riemann problem is quite complicated: For each phase, one has four possible configurations (rarefaction/shock, shock/rarefaction, rarefaction/rarefaction, shock/shock) with a contact discontinuity in the center. The waves of the different phases can overlap arbitrarily with each other.

Our main interest in the exact solution to the Riemann problem is to get a benchmark for testing of numerical schemes. Therefore, instead of solving the “direct” Riemann problem, we can perform what we call the “inverse” Riemann problem: Given some intermediate state $\mathbf{u}_0$ and the configuration of the Riemann problem, one finds the end states $\mathbf{u}_L, \mathbf{u}_R$, which can be connected to $\mathbf{u}_0$ by the admissible waves. In doing so, we are able to construct the exact solution for Riemann problems, see Section 3. Now, we can use the obtained exact solution as benchmark problems, see Section 8. Note that in constructing the exact solution we can easily get some interesting configurations, e.g. with coinciding waves, see Section 6.

The paper is organized as follows. In Section 2, we present the mathematical model. In Section 3, we present the construction of the exact solution of the Riemann problem. It appears that the non-conservative effects play a role only across one wave in the solution of the Riemann problem, the solid contact wave. Section 4 is devoted to investigating its properties. In Section 5 we show that under certain conditions, the gas part of the governing equations for the BN model reveals the system of the Euler equations in the duct of variable cross section. Also, we study the analogy between the flow across the solid contact and the classical converging–diverging Laval nozzle. Section 6 is devoted to the cases when some of the waves in the solution of the Riemann problem approach each other. In Section 7 we note that for the Riemann problem, the original *non-conservative* system of governing equations is equivalent to some *conservative* system locally. This allows us to introduce the notion of a weak solution for the Riemann problem. Finally, in Section 8 we propose some test problems, based on the exact solution of the Riemann problem. To assess the performance of numerical methods on these tests, we use the method for compressible multiphase flows which we have proposed recently, see [1], and discuss the results.

2 Mathematical model

In this work, we consider only the non-viscous flows without mass, heat transfer and wall friction. Moreover, we restrict ourselves to one-dimensional flow. Denote the two phases with subscripts a and b, respectively. Since the BN model describes the flame spread and the deflagration-to-detonation transition (DDT) in gas-permeable solids, see [2], we will call the phase a *solid*, and phase b *gas*. Let ρ_k be the density, u_k the velocity, p_k the pressure, E_k the total specific energy, and α_k the volume fraction of the phase $k = a, b$. Then, the system of governing equations for the two-phase flow will be [2]

$$\begin{aligned}
\frac{\partial \alpha_a}{\partial t} + u_a \frac{\partial \alpha_a}{\partial x} &= 0 \\
\frac{\partial \alpha_a \rho_a}{\partial t} + \frac{\partial \alpha_a \rho_a u_a}{\partial x} &= 0 \\
\frac{\partial \alpha_a \rho_a u_a}{\partial t} + \frac{\partial (\alpha_a \rho_a u_a^2 + \alpha_a p_a)}{\partial x} &= +p_b \frac{\partial \alpha_a}{\partial x} \\
\frac{\partial \alpha_a \rho_a E_a}{\partial t} + \frac{\partial \alpha_a u_a (\rho_a E_a + p_a)}{\partial x} &= +p_b u_a \frac{\partial \alpha_a}{\partial x} \\
\frac{\partial \alpha_b \rho_b}{\partial t} + \frac{\partial \alpha_b \rho_b u_b}{\partial x} &= 0 \\
\frac{\partial \alpha_b \rho_b u_b}{\partial t} + \frac{\partial (\alpha_b \rho_b u_b^2 + \alpha_b p_b)}{\partial x} &= -p_b \frac{\partial \alpha_a}{\partial x} \\
\frac{\partial \alpha_b \rho_b E_b}{\partial t} + \frac{\partial \alpha_b u_b (\rho_b E_b + p_b)}{\partial x} &= -p_b u_a \frac{\partial \alpha_a}{\partial x}.
\end{aligned} \tag{2.1}$$

We assume that each phase is described by the Stiffened gas equation of state (EOS), i.e.,

$$e_k = \frac{p_k + \gamma_k \pi_k}{\rho_k (\gamma_k - 1)}, \qquad k = a, b, \tag{2.2}$$

where γ_k, π_k are the constants, specific for the phase k. To close the system (2.1), we use the saturation constraint

$$\alpha_a + \alpha_b = 1.$$

Remark 2.1. In comparison to [2], we have excluded the non-differential source terms, which appear in [2] and describe the compaction rate, residual momentum and energy exchange. Also, we assume that the internal energy e_k does not depend on α_a, as it does in [2]. The reason for all these simplifications is that we are mostly interested in treating of the differential properties of (2.1), and they are unaffected by these assumptions.

An important feature of the system (2.1) is the presence of the so-called *non-conservative terms*. These are the terms

$$\pm p_b \frac{\partial \alpha_a}{\partial x}, \qquad \pm p_b u_a \frac{\partial \alpha_a}{\partial x} \tag{2.3}$$

on the right hand side of (2.1), and the transport equation for the volume fraction. Due to these terms, the system (2.1) cannot be written in divergence form. Consequently, the notion of weak solution cannot be defined for (2.1) in the usual manner. Note that for the case $\alpha_a = \text{const}$, the system decouples into the two sets Euler equations for the phases a and b. For the mixture, one can get the *conservative* balance equations by summing the corresponding single-phase equations.

A mathematical analysis of the BN model was carried out by Embid and Baer [6]. They found that the eigenvalues of the system are

$$\begin{aligned} &\lambda_1 = u_a, \\ &\lambda_2 = u_a - c_a, \quad \lambda_3 = u_a, \quad \lambda_4 = u_a + c_a, \\ &\lambda_5 = u_b - c_b, \quad \lambda_6 = u_b, \quad \lambda_7 = u_b + c_b, \end{aligned} \tag{2.4}$$

where $c_k = \sqrt{\gamma_k(p_k + \pi_k)/\rho_k}$ is the sound speed, $k = a, b$. The 2, 4, 5, and 7 characteristic fields are genuinely nonlinear, and the others are linearly degenerate. The system (2.1) is hyperbolic, although not strictly hyperbolic. Indeed, situations are possible, when some of the eigenvalues of the solid phase can coincide with some of the gas phase. Also, u_a is the double eigenvalue. In [6], it was shown that the eigenvectors of the system become linearly dependent in the points in the flow, where any one of conditions

$$\alpha_a = 0, \quad \alpha_b = 0, \quad c_b^2 - (u_b - u_a)^2 = 0 \tag{2.5}$$

holds. In this case, a parabolic degeneracy occurs. In what follows, we will always consider two-phase *mixtures*, i.e. the case of pure liquids will be excluded. The case $c_b^2 - (u_b - u_a)^2 = 0$ will be addressed in Subsection 6.2.

The characteristic analysis of Embid and Baer [6] shows that the Riemann invariants for the 2–7 characteristic fields coincide with those for the Euler equations for the phases $k = a, b$, the gas parameters do not change across the solid waves and vice versa. Also, $\alpha_a = \text{const}$ across the 2-7 characteristic fields. As we have mentioned above, then the system (2.1) decouples into the two sets of Euler equations for the phases a and b, the fact which we will use in Section 7 to introduce the notion of a weak solution for the Riemann problem. Across the

1st characteristic field, the Riemann invariants are

$$\begin{aligned}
\psi_a &= u_a \\
\psi_b &= \eta_b \\
\psi_3 &= \alpha_b \rho_b (u_a - u_b) \\
\psi_4 &= \alpha_a p_a + \alpha_b p_b + \alpha_b \rho_b (u_a - u_b)^2 \\
\psi_5 &= \frac{(u_a - u_b)^2}{2} + h_b,
\end{aligned} \tag{2.6}$$

where $\eta_b = (p_b + \pi_b)/\rho_b^{\gamma_b}$ is the isentrope and h_b is the specific enthalpy of the phase b, see [6] for details.

3 Exact solution to the Riemann problem

Let us rewrite the system (2.1) in primitive variables and consider the Riemann problem for it, i.e.,

$$\frac{\partial \mathbf{u}}{\partial t} + \mathbf{A}(\mathbf{u}) \frac{\partial \mathbf{u}}{\partial x} = 0, \tag{3.1}$$

with

$$\mathbf{A} = \begin{bmatrix}
u_a & 0 & 0 & 0 & 0 & 0 & 0 \\
0 & u_a & \rho_a & 0 & 0 & 0 & 0 \\
\frac{p_a - p_b}{\alpha_a \rho_a} & 0 & u_a & 1/\rho_a & 0 & 0 & 0 \\
0 & 0 & \rho_a c_a^2 & u_a & 0 & 0 & 0 \\
-\frac{\rho_b}{\alpha_b}(u_b - u_a) & 0 & 0 & 0 & u_b & \rho_b & 0 \\
0 & 0 & 0 & 0 & 0 & u_b & 1/\rho_b \\
-\frac{\rho_b c_b^2}{\alpha_b}(u_b - u_a) & 0 & 0 & 0 & 0 & \rho_b c_b^2 & u_b
\end{bmatrix}, \quad \mathbf{u} = \begin{bmatrix} \alpha_a \\ \rho_a \\ u_a \\ p_a \\ \rho_b \\ u_b \\ p_b \end{bmatrix}, \tag{3.2}$$

and the initial data

$$\mathbf{u}(x, 0) = \begin{cases} \mathbf{u}_L, & x \leq 0 \\ \mathbf{u}_R, & x > 0. \end{cases} \tag{3.3}$$

Since there are six distinct eigenvalues, cf. (2.4), there are at most seven intermediate states in the solution of the Riemann problem. The usual "direct" solution of the Riemann problem is found as follows: Given the end states $\mathbf{u}_L, \mathbf{u}_R$, one has to find the intermediate states. However, it is problematic to find it for the two-phase model, since the structure of the Riemann problem is quite complicated: For each phase, one has four possible configurations (rarefaction/shock, shock/rarefaction, rarefaction/rarefaction, shock/shock), and the waves can overlap with each other.

Our main interest in the exact solution to a Riemann problem is to get a benchmark for testing of numerical schemes. Therefore, instead of solving the "direct" Riemann problem, we can look at what we call the "inverse" Riemann

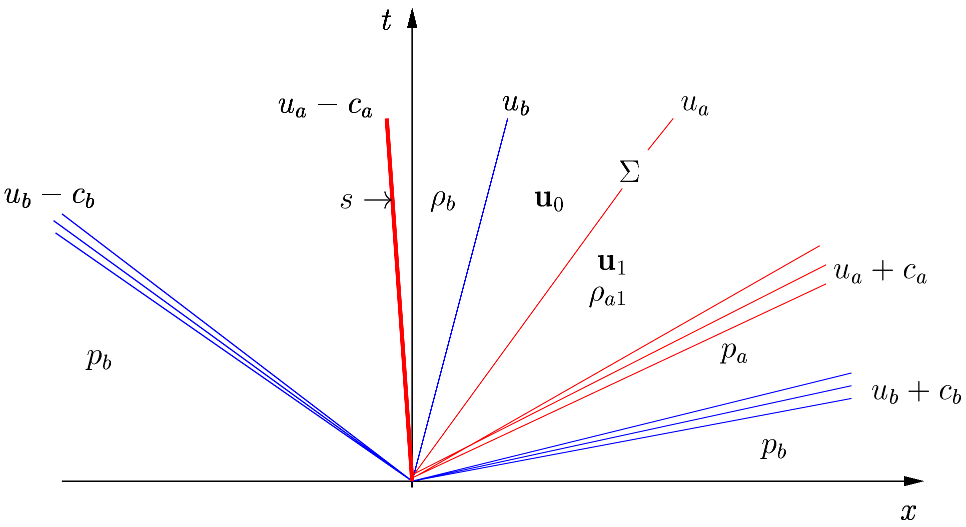

Figure 1: "Inverse" solution of the Riemann problem.

problem: Given some intermediate state $\mathbf{u}_0$ and the configuration of the Riemann problem, one finds end states $\mathbf{u}_L, \mathbf{u}_R$, which can be connected to $\mathbf{u}_0$ by the admissible waves.

Let us concretize the procedure of the "inverse" solution, see Fig. 1. We choose the intermediate state $\mathbf{u}_0$ at the left to the solid contact Σ, and fix the volume fractions to the left and to the right of Σ. Given also the configuration, which means that we prescribe, which waves should be at the left of Σ, and which to the right. Depending on the wave, we determine the position of the wave by specifying the following quantities

- Shock: given shock speed, family
- Rarefaction: given pressure behind, family
- Contact: given density behind

For now, we make the assumption that the solid contact Σ with speed u_a does not coincide with any other wave. Therefore, we can use the usual Rankine-Hugoniot conditions across the shocks. Then, using the configuration data, for each wave we can find the state behind it. For the case of coinciding wave speeds, see Section 6.

It appears that across the solid contact Σ the solution is not trivial. In the following we denote the state left to the solid contact by the subscript 0 and the right state by 1. The solid particle speed invariants are

$$u_{a0} = u_{a1} = u_a \tag{3.4a}$$

$$\eta_{b0} = \eta_{b1} = \eta_b \tag{3.4b}$$

$$\alpha_{b0}\rho_{b0}(u_{b0} - u_a) = \alpha_{b1}\rho_{b1}(u_{b1} - u_a) = M \tag{3.4c}$$

$$\alpha_{a0}p_{a0} + \alpha_{b0}p_{b0} + \alpha_{b0}\rho_{b0}(u_{b0} - u_a)^2 = \alpha_{a1}p_{a1} + \alpha_{b1}p_{b1} + \alpha_{b1}\rho_{b1}(u_{b1} - u_a)^2 = P \tag{3.4d}$$

$$\frac{(u_{b0} - u_a)^2}{2} + h_{b0} = \frac{(u_{b1} - u_a)^2}{2} + h_{b1} = E. \tag{3.4e}$$

Here

$$\eta_b = \frac{p_b + \pi_b}{\rho_b^{\gamma_b}}, \qquad h_b = \frac{\gamma_b(p_b + \pi_b)}{\rho_b(\gamma_b - 1)}$$

are respectively the entropy and the enthalpy of the gas phase, subscripts 0 and 1 denote the states to the left and the right of Σ. Note that the solid density ρ_a does not appear in (3.4), it acts as a free parameter. Note also, that the system (3.4) is an *undetermined* system for the parameters at the left and at the right of the solid contact. Indeed, we have 14 unknowns

$$\alpha_{ai}, \rho_{ai}, u_{ai}, p_{ai}, \rho_{bi}, u_{bi}, p_{bi}, \qquad i = 0, 1,$$

but only 5 equations. Therefore, one has to fix 9 unknowns. We choose to fix the following variables

$$\alpha_{a0}, \rho_{a0}, u_{a0}, p_{a0}, \rho_{b0}, u_{b0}, p_{b0}, \alpha_{a1}, \rho_{a1}.$$

Then, the number of the equations in (3.4) and the number of unknowns coincide and one might hope to get a solution.

Note that the system (3.4) is reminiscent of the mass, momentum, and energy balance across a discontinuity, propagating with the speed u_a, for the Euler equations for the gas phase. Consider the case

$$\alpha_{b0} = \alpha_{b1},$$

and the other parameters keep their values. Remember that this corresponds to the decoupled Euler equations for the gas and solid phases, see the system (2.1). So, the gas flow does not see the solid phase, and obviously the gas parameters do not change across u_a. Thus, there always exists the trivial solution

$$\begin{aligned} \rho_{b0} &= \rho_{b1} \\ u_{b0} &= u_{b1} \\ p_{b0} &= p_{b1}. \end{aligned} \tag{3.5}$$

Note that this is the unique *admissible* solution of (3.4). In what follows, we will refer to this case as "Euler", and the case

$$\alpha_{b0} \neq \alpha_{b1}$$

as "multiphase". In what follows, we will often fix the phase variables ρ_k, u_k, p_k, $k = a, b$, and consider the Euler case $\alpha_{b0} = \alpha_{b1}$ and the multiphase case $\alpha_{b0} \neq \alpha_{b1}$. If we let

$$\frac{\alpha_{b0}}{\alpha_{b1}} \to 1,$$

then the multiphase case will turn into the Euler case.

Combining the equations of (3.4), we get the following nonlinear equation for the gas density to the right of u_a

$$F(\rho_{b1}) = \frac{1}{2}\left(\frac{M}{\alpha_{b1}\rho_{b1}}\right)^2 + \frac{\gamma_b \eta_b \rho_{b1}^{\gamma_b - 1}}{\gamma_b - 1} - E = 0. \tag{3.6}$$

The derivative of $F(\rho)$ is

$$F'(\rho) = -\frac{M^2}{\alpha_{b1}^2 \rho^3} + \gamma_b \eta_b \rho^{\gamma_b - 2}. \tag{3.7}$$

At the point ρ_*, the function $F(\rho)$ reaches its minimum

$$\rho_* = \left(\frac{M^2}{\alpha_{b1}^2 \gamma_b \eta_b}\right)^{\frac{1}{\gamma_b + 1}}. \tag{3.8}$$

Indeed, for all $\rho < \rho_*$ we have

$$\rho^{\gamma_b + 1} < \rho_*^{\gamma_b + 1} = \frac{M^2}{\alpha_{b1}^2 \gamma_b \eta_b},$$

giving

$$\gamma_b \eta_b \rho^{\gamma_b - 2} < \frac{M^2}{\alpha_{b1}^2 \rho^3}.$$

Consequently,

$$F'(\rho) < 0$$

for all $\rho < \rho_*$. Analogously,

$$F'(\rho) > 0$$

for all $\rho > \rho_*$. Note also that $F(\rho) \to +\infty$ as $\rho \to +0$ or $\rho \to +\infty$.

Depending on the sign of $F(\rho_{b1})$, the equation (3.6) can have no, one, or two roots. We will investigate each case separately.

3.1 No roots

Consider the solid particle speed invariants (3.4). We will fix the left state 0, and look for the root of the equation (3.6) for the variable right gas volume fraction α_{b1}.

We can rewrite (3.4c) as

$$\rho_{b0}(u_{b0} - u_a) = \frac{\alpha_{b1}}{\alpha_{b0}}\rho_{b1}(u_{b1} - u_a) = \frac{M}{\alpha_{b0}} = M_E,$$

where the subscript E stands for Euler. Indeed, M_E is equal to the mass flow for the Euler case $\alpha_{b0} = \alpha_{b1}$. With a *constant* α_{b0}, we have the constant M_E at the right hand side.

Let us rewrite the equation (3.6) as follows,

$$F(\rho_{b1}) = \frac{1}{2}M_E^2\left(\frac{\alpha_{b0}}{\alpha_{b1}}\right)^2\frac{1}{\rho_{b1}^2} + \frac{\gamma_b\eta_b\rho_{b1}^{\gamma_b-1}}{\gamma_b - 1} - E = 0. \tag{3.9}$$

For the Euler case

$$\frac{\alpha_{b0}}{\alpha_{b1}} = 1$$

and (3.9) always has at least one trivial solution (3.5). For variable $\alpha_{b1} \in]0,1[$ (multiphase case), we have

$$\frac{\alpha_{b0}}{\alpha_{b1}} \in]\alpha_{b0}, \infty[.$$

It is obvious that if for some positive A, A big enough,

$$\frac{\alpha_{b0}}{\alpha_{b1}} > A, \tag{3.10}$$

then (3.9) has no roots, since $E, \eta_b, \rho_b > 0$ and $\gamma_b > 1$. Thus for all α_{b1}, $\alpha_{b1} < \alpha_{b0}/A$, the equation (3.9) has no roots. Decreasing α_{b1} (or increasing α_{a1}, $\alpha_{a1} = 1 - \alpha_{b1}$), one necessarily gets no solution for some value of α_{b1}.

3.2 One or two roots

Consider again the equations

$$F(\rho_{b1}) = \frac{1}{2}\left(\frac{M}{\alpha_{b1}\rho_{b1}}\right)^2 + \frac{\gamma_b\eta_b\rho_{b1}^{\gamma_b-1}}{\gamma_b - 1} - E = 0 \tag{3.11}$$

$$F'(\rho) = -\frac{M^2}{\alpha_{b1}^2\rho^3} + \gamma_b\eta_b\rho^{\gamma_b-2}. \tag{3.12}$$

Suppose first that (3.11) has two roots. Denote them $\tilde{\rho}_{b1}$, $\tilde{\tilde{\rho}}_{b1}$,

$$\tilde{\rho}_{b1} < \tilde{\tilde{\rho}}_{b1}.$$

Then

$$F'(\tilde{\rho}_{b1}) < 0, \qquad F'(\tilde{\tilde{\rho}}_{b1}) > 0.$$

Using (3.4c)

$$\frac{M^2}{\alpha_{b1}^2} = (u_{b1} - u_a)^2 \rho_{b1}^2$$

we can rewrite (3.12) as

$$-(u_{b1} - u_a)^2 + c_{b1}^2 = F'(\rho_{b1})\rho_{b1}, \tag{3.13}$$

where $c_{b1}^2 = \gamma_b(p_{b1} + \pi_b)/\rho_{b1}$ is the gas sound speed squared. We see that the volume fraction α_b does not appear in this equation. This means that it should hold for any values of α_{b0}, α_{b1} on both sides of Σ. In particular, for the Euler case $\alpha_{b0} = \alpha_{b1}$, the admissible solution is (3.5),

$$\begin{aligned} \rho_{b0} &= \rho_{b1} \\ u_{b0} &= u_{b1} \\ p_{b0} &= p_{b1}. \end{aligned}$$

Thus, we have the two roots $\tilde{\rho}_{b1}$, $\tilde{\tilde{\rho}}_{b1}$ of (3.11) as candidates for ρ_{b1}. We choose the one for which

$$\operatorname{sign}(-(u_{b0} - u_a)^2 + c_{b0}^2) = \operatorname{sign}(-(u_{b1} - u_a)^2 + c_{b1}^2) \tag{3.14}$$

since all these quantities are identical on the left and right side. By (3.13), it is equivalent to the condition

$$\operatorname{sign}(F'(\rho_{b0})) = \operatorname{sign}(F'(\rho_{b1})). \tag{3.15}$$

For the multiphase case $\alpha_{b0} \neq \alpha_{b1}$, we also choose by a continuity argument the root of (3.11), which satisfies the condition (3.15). It corresponds to the admissible root for the Euler case, if α_{b1} would be equal to α_{b0}.

Physically, this choice has the following meaning. Consider the Euler case $\alpha_{b0} = \alpha_{b1}$, and let the admissible Euler root be $\tilde{\rho}_{b1}$. Then, it satisfies the criterion (3.15). Now let us deviate the ratio α_{b0}/α_{b1} slightly, i.e,

$$\frac{\alpha_{b0}}{\alpha_{b1}} := 1 + \epsilon, \quad \epsilon \text{ small.}$$

Then, for this *multiphase* case the admissible root is also $\tilde{\rho}_{b1}$, it cannot suddenly become $\tilde{\tilde{\rho}}_{b1}$. We summarize these ideas by formulating the following definition.

Definition 3.1. *The physically admissible state behind the solid contact is determined by the root of* (3.6), *which satisfies the condition* (3.15).

The case of the single root of (3.11) corresponds to the degenerate situation, when the gas velocity relative to u_a is sonic to the right of Σ, i.e., $|u_{b1} - u_a| = c_{b1}$. See also Subsection 6.2 below.

4 Properties of the solid contact

Consider the solution of the system (3.1), consisting of a single solid contact Σ, propagating with the speed u_a. Denote the states to the left and right of it by $\mathbf{u}_0$ and $\mathbf{u}_1$, respectively. Let us investigate, under which conditions this discontinuity will be well posed.

We can linearize the system of governing equations (3.1) on the both sides of Σ, i.e., assume $\mathbf{u} = \mathbf{u}_0 + \tilde{\mathbf{u}}$ at the left, and $\mathbf{u} = \mathbf{u}_1 + \tilde{\tilde{\mathbf{u}}}$ at the right. Then, the small perturbations $\tilde{\mathbf{u}}$ and $\tilde{\tilde{\mathbf{u}}}$ must satisfy the linear systems

$$\frac{\partial \tilde{\mathbf{u}}}{\partial t} + \mathbf{A}(\mathbf{u}_0)\frac{\partial \tilde{\mathbf{u}}}{\partial x} = 0, \qquad \frac{\partial \tilde{\tilde{\mathbf{u}}}}{\partial t} + \mathbf{A}(\mathbf{u}_1)\frac{\partial \tilde{\tilde{\mathbf{u}}}}{\partial x} = 0 \tag{4.1}$$

to second order of accuracy. Assume that the systems (4.1) are diagonalisable, i.e., we can introduce the characteristic variables $\mathbf{w} = \mathbf{R}^{-1}\mathbf{u}$, $\mathbf{R}$ is the matrix of right eigenvectors of $\mathbf{A}$. By (2.5), we know that the transformation $\mathbf{u} \mapsto \mathbf{w}$ exists as long as $(u_b - u_a)^2 - c_b^2 \neq 0$. For now, we will be dealing only with this case. The case when $(u_b - u_a)^2 - c_b^2 = 0$ is considered in Section 6.2.

By changing to characteristic variables on the both sides of Σ, the two systems split into $2p$, $p = 7$, scalar equations

$$\frac{\partial \tilde{w}_i}{\partial t} + \lambda_i(\mathbf{u}_0)\frac{\partial \tilde{w}_i}{\partial x} = 0, \qquad \frac{\partial \tilde{\tilde{w}}_i}{\partial t} + \lambda_i(\mathbf{u}_1)\frac{\partial \tilde{\tilde{w}}_i}{\partial x} = 0, \tag{4.2}$$

where $i = 1, \ldots, p$ and λ_i are the eigenvalues of $\mathbf{A}$ at the state $\mathbf{u}_0$ and $\mathbf{u}_1$. Thus, small disturbances propagate with the characteristic speeds λ_i. We can subdivide these characteristics into

(I) incoming: $\lambda_i(\mathbf{u}_0) > u_a$, $\lambda_i(\mathbf{u}_1) < u_a$

(II) coinciding: $\lambda_i(\mathbf{u}_0) = u_a$, $\lambda_i(\mathbf{u}_1) = u_a$

(III) outgoing: $\lambda_i(\mathbf{u}_0) < u_a$, $\lambda_i(\mathbf{u}_1) > u_a$.

The relations along the incoming and coinciding characteristics are fully determined from the initial data, i.e. from the "past". The data prescribed on Σ determines the outgoing characteristics. This gives rise to the following definition.

Definition 4.1. *Consider a discontinuity Σ such that the number of outgoing characteristics is s, and the number of relations across Σ is m. Then Σ is called evolutionary, if*

$$s + 1 = m.$$

Remark 4.2. This definition leaves one degree of freedom for the propagation speed. The definition is based on the discussion in Landau and Lifshitz [10, §88], see also Kulikovskii et. al. [9].

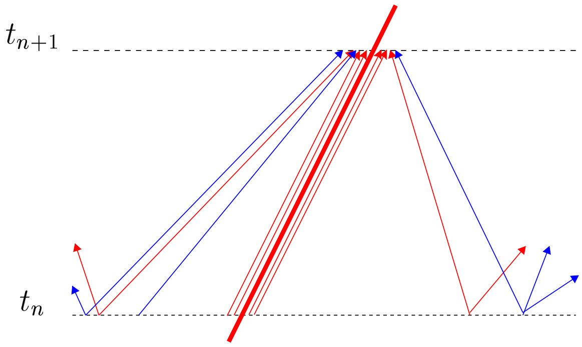

Figure 2: Solid-related characteristics around the solid contact.

On the other hand, if there are N unknowns on the discontinuity Σ, including its speed, there should be also N conditions for them, in order for the discontinuity be specified. Some of these conditions are given by the incoming and coinciding characteristics. Additional conditions are obtained from the relations across the discontinuity. The following theorem makes use of these considerations.

Theorem 4.3. *Consider a discontinuity Σ in the solution to a system of p equations, such that the number of unknowns on it is N. Denote the number of the incoming and coinciding characteristics by n, and the number of relations across Σ by m. Then Σ is evolutionary, if*

$$N = n + m.$$

Proof. Since the order of the system of governing equations (2.1) is p, then there are p characteristics on the either side of Σ, so the total number of characteristics is $2p$. Then $s = 2p - n$, where s is the number of outcoming characteristics. On the discontinuity Σ, there are p unknowns on the either side of it, and the speed of Σ itself, so $N = 2p + 1$. Using this in Definition 4.1, one gets the desired result. □

Using this theorem, we can point out when the solid contact will be evolutionary.

Theorem 4.4. *The solid contact in system* (2.1) *is evolutionary, if there are precisely 3 gas-related incoming characteristics on it.*

Proof. Since $p = 7$, there are $N = 15$ unknowns on the solid contact. There are 6 solid-related incoming or coinciding characteristics: u_{a0}, u_{a0}, u_{a1}, u_{a1} (u_a is a double eigenvalue), $u_{a0} + c_{a0}$, and $u_{a1} - c_{a1}$, see Fig. 2. Across the solid contact, the 5 relations (3.4) hold. Finally, the speed of the solid contact is u_a. Therefore, we have $m = 6$. By Theorem 4.3,

$$15 = 6 + n_b + 6,$$

where n_b is the number of gas-related incoming characteristics. Thus $n_b = 3$. □

Remark 4.5. In the formulation of the "inverse" problem in Section 3, the unknowns on the solid contact are

$$\underbrace{\rho_{a0}, u_{a0}, p_{a0}, \rho_{a1}, \alpha_{a0}, \alpha_{a1},}_{\substack{\text{from 6 incoming or coinciding} \\ \text{solid characteristics}}} \quad \underbrace{\rho_{b0}, u_{b0}, p_{b0},}_{\substack{\text{from 3 incoming} \\ \text{gas characteristics}}} \quad \underbrace{u_{a1}, p_{a1},}_{\substack{\text{for 2 outcoming} \\ \text{solid characteristics}}} \quad \underbrace{\rho_{b1}, u_{b1}, p_{b1},}_{\substack{\text{for 3 outcoming} \\ \text{gas characteristics}}}$$

i.e., there are 6 solid variables, which are assumed to be known from the solid-related impinging characteristics, and 3 gas variables from the gas characteristics. The remaining 5 unknowns are found from the solution of the 5 equations (3.4) as described in Section 3.

Next, we prove that the physically admissible state behind the solid contact, see Section 3, implies that the solid contact is an evolutionary discontinuity. Namely, the following statement holds.

Theorem 4.6. *The physically admissible root of* (3.6) *determines the state behind the solid contact, such that precisely three gas-related characteristics impinge on the solid contact from the both sides.*

Proof. From the constancy of the third Riemann invariant across the solid contact, i.e. from (3.4c), it follows that

$$u_{b0} < u_a \Leftrightarrow u_{b1} < u_a.$$

Analogously,

$$u_{b0} > u_a \Leftrightarrow u_{b1} > u_a.$$

We prove the above statement by considering the different cases in the equation (3.14). We consider the three gas-related characteristics

$$\lambda_5 = u_b - c_b < \lambda_6 = u_b < \lambda_7 = u_b + c_b.$$

I.		$u_{b0} > u_a$	$u_{b1} > u_a$
	A.	$-(u_{b0} - u_a)^2 + c_{b0}^2 > 0$ $\Leftrightarrow \lvert u_{b0} - u_a \rvert < c_{b0}$ $\Leftrightarrow u_{b0} - c_{b0} < u_a$ 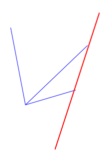	$-(u_{b1} - u_a)^2 + c_{b1}^2 > 0$ $\Leftrightarrow \lvert u_{b1} - u_a \rvert < c_{b1}$ $\Leftrightarrow u_{b1} - c_{b1} < u_a$ 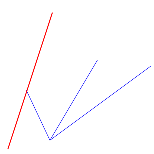
	B.	$-(u_{b0} - u_a)^2 + c_{b0}^2 < 0$ $\Leftrightarrow \lvert u_{b0} - u_a \rvert > c_{b0}$ $\Leftrightarrow u_{b0} - c_{b0} > u_a$ 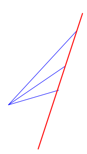	$-(u_{b1} - u_a)^2 + c_{b1}^2 < 0$ $\Leftrightarrow \lvert u_{b1} - u_a \rvert > c_{b1}$ $\Leftrightarrow u_{b1} - c_{b1} > u_a$ 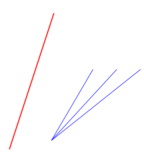

II.		$u_{b0} < u_a$	$u_{b1} < u_a$
	A.	$-(u_{b0}-u_a)^2 + c_{b0}^2 > 0$ $\Leftrightarrow \lvert u_{b0}-u_a\rvert < c_{b0}$ $\Leftrightarrow u_{b0}+c_{b0} > u_a$ 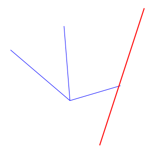	$-(u_{b1}-u_a)^2 + c_{b1}^2 > 0$ $\Leftrightarrow \lvert u_{b1}-u_a\rvert < c_{b1}$ $\Leftrightarrow u_{b1}+c_{b1} > u_a$ 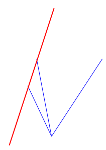
	B.	$-(u_{b0}-u_a)^2 + c_{b0}^2 < 0$ $\Leftrightarrow \lvert u_{b0}-u_a\rvert > c_{b0}$ $\Leftrightarrow u_{b0}+c_{b0} < u_a$ 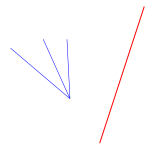	$-(u_{b1}-u_a)^2 + c_{b1}^2 < 0$ $\Leftrightarrow \lvert u_{b1}-u_a\rvert > c_{b1}$ $\Leftrightarrow u_{b1}+c_{b1} < u_a$ 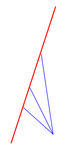

The above figures illustrate the four possibilities for the mutual position of the gas-related characterics on both sides of the solid contact, giving the result. □

Remark 4.7. This theorem is analogous to the derivation of the Lax shock conditions for the system of the conservation laws, see e.g. Smoller [13].

Remark 4.8. In the proof of Theorem 4.6, we did not consider the case when the solid velocity u_a coincides with any other characteristic speed. We leave this question until Section 6.

Using Theorem 4.6, we can introduce the following definitions.

Definition 4.9. *The solid contact is called* admissible, *if precisely three gas-related characteristics impinge on it from the both sides.*

Definition 4.10. *The side of the solid contact through which the gas enters is called the front side, while the other side is called the back side.*

Remark 4.11. Note that the Definition 4.10 makes sense: For the admissible solid contact, the gas may enter the solid contact only from one side. To see this, consider the different cases in the proof of Theorem 4.6.

From Theorems 4.3 and 4.6 it follows that on the both sides of the solid contact, all unknowns are determined for all $t > 0$. Therefore, we can consider the solid contact as a boundary, and formulate initial boundary value problems (IBVP) for the systems (4.1) (or, equivalently (4.2)) on the both sides of it. Without loss of generality, we can assume that the eigenvalues of $\mathbf{A}(\mathbf{u}_0)$ and $\mathbf{A}(\mathbf{u}_1)$

are ordered increasing. Denote the number of outgoing characteristics to the left of the solid contact by s_0, and to the right of it by s_1. Then

$$
\begin{aligned}
\lambda_1(\mathbf{u}_0) \le \cdots \le \lambda_{s_0}(\mathbf{u}_0) < u_a \le \lambda_{s_0+1}(\mathbf{u}_0) \le \cdots \le \lambda_p(\mathbf{u}_0)\\
\lambda_1(\mathbf{u}_1) \le \cdots \le \lambda_{p-s_1}(\mathbf{u}_1) \le u_a < \lambda_{p-s_1+1}(\mathbf{u}_1) \le \cdots \le \lambda_p(\mathbf{u}_1).
\end{aligned}
$$

Since Σ is evolutionary, precisely s_0 parameters are given at the left of Σ, and s_1 at the right of it. We can interpret these *known* parameters as the boundary conditions for the following *linear* IBVPs at the left and at the right of Σ, respectively:

$$
\frac{\partial \tilde{w}_i}{\partial t} + \lambda_i(\mathbf{u}_0)\frac{\partial \tilde{w}_i}{\partial x} = 0, \quad
\begin{array}{l}
\tilde{w}_1, \ldots, \tilde{w}_{s_0} \text{ are prescribed on } \Sigma\\
\tilde{w}_{s_0+1}, \ldots, \tilde{w}_p \text{ are prescribed at } t = 0
\end{array}
\tag{4.3}
$$

$$
\frac{\partial \tilde{\tilde{w}}_i}{\partial t} + \lambda_i(\mathbf{u}_1)\frac{\partial \tilde{\tilde{w}}_i}{\partial x} = 0, \quad
\begin{array}{l}
\tilde{\tilde{w}}_1, \ldots, \tilde{\tilde{w}}_{p-s_1} \text{ are prescribed at } t = 0\\
\tilde{\tilde{w}}_{p-s_1+1}, \ldots, \tilde{\tilde{w}}_p \text{ are prescribed on } \Sigma.
\end{array}
\tag{4.4}
$$

The IBVPs (4.3) and (4.4) imply that $\tilde{w}_i$ and $\tilde{\tilde{w}}_i$ are constant along the characteristics $\lambda_i(\mathbf{u}_0)$ and $\lambda_i(\mathbf{u}_1)$ respectively, and the initial values for $\tilde{w}_i$ and $\tilde{\tilde{w}}_i$ are given. Obviously, the IBVPs (4.3) and (4.4) are well-posed and have unique solutions. Thus, we have the following theorem.

Theorem 4.12. *The solid contact is evolutionary iff the linear IBVPs* (4.3) *and* (4.4) *are well-posed and have unique solutions.*

Remark 4.13. A nice interpretation of the admissibility of the solid contact can be obtained, if we consider the entropy as the *measure of the information* of the system. By the second law of thermodynamics, the entropy increases at shocks, which characterizes irreversible processes. The states behind the shock do not know anything about the upstream flow. In other words, the state behind the shock possesses less information on the flow than the state before the shock, i.e., the information is lost. Geometrically, the admissible shocks are described by the intersection of of the characteristics of the same family (Lax shock inequalities). Therefore, we can say that the lost of information is caused by the intersection of the characteristics of the same family.

In this light, consider the admissible solid contact. Across it, the gas entropy does not change, cf. the second equation of (3.4). One can easily see that the gas-related characteristics of the same family do not impinge on the both sides of the solid contact, cf. the different cases in the proof of Theorem 4.6. Therefore, we state that the *information across the solid contact is not lost.*

5 Gas dynamics analogy

It has been recognized by several authors [3, 12] that the form of the governing equations of the two-phase flow (2.1) is reminiscent of the Euler equations in the duct of variable cross section $A = A(x)$,

$$\begin{aligned} \frac{\partial A\rho}{\partial t} + \frac{\partial A\rho v}{\partial x} &= 0 \\ \frac{\partial A\rho v}{\partial t} + \frac{\partial A(\rho v^2 + p)}{\partial x} &= p\frac{\partial A}{\partial x} \\ \frac{\partial A\rho E}{\partial t} + \frac{\partial Av(\rho E + p)}{\partial x} &= 0. \end{aligned} \tag{5.1}$$

For the derivation, see e.g. Zucrow and Hoffman [17]. Usually, the cross-section $A = A(x)$ is assumed to be *a priori* given. However, we can consider it as an additional unknown, and supply the trivial equation $A_t = 0$ for determining it. Thus, the system (5.1) becomes

$$\frac{\partial A}{\partial t} = 0 \tag{5.2a}$$

$$\frac{\partial A\rho}{\partial t} + \frac{\partial A\rho v}{\partial x} = 0 \tag{5.2b}$$

$$\frac{\partial A\rho v}{\partial t} + \frac{\partial A(\rho v^2 + p)}{\partial x} = p\frac{\partial A}{\partial x} \tag{5.2c}$$

$$\frac{\partial A\rho E}{\partial t} + \frac{\partial Av(\rho E + p)}{\partial x} = 0. \tag{5.2d}$$

Note that this system can be formally obtained from the system of governing equations for the two-phase flow (2.1), if one sets there

$$\begin{aligned} \rho_a &\equiv \text{const} \\ u_a &\equiv 0 \\ p_a &\equiv \text{const.} \end{aligned}$$

Then, the gas volume fraction α_b in (2.1) plays the role of the cross section A in (5.2), and the gas part of (2.1) recovers the system (5.2). Consequently, one can construct the exact solution to the Riemann problem for the system (5.2) exactly as it was done in Section 3 for the system of the two-phase flow equations (2.1). One just has to set the solid velocity equal to zero, and consider the Riemann problem, consisting only of gas waves. In doing so, we can get test cases for numerical methods for the Euler equations in the duct of variable cross section. See Section 8 for an example.

The Riemann problem for (5.2) is determined by fixing some left and right states A_0, ρ_0, v_0, p_0 and A_1, ρ_1, v_1, p_1. It can be viewed as the decay of the initial discontinuity in the tube with the sudden change in the cross-section, see Fig. 3.

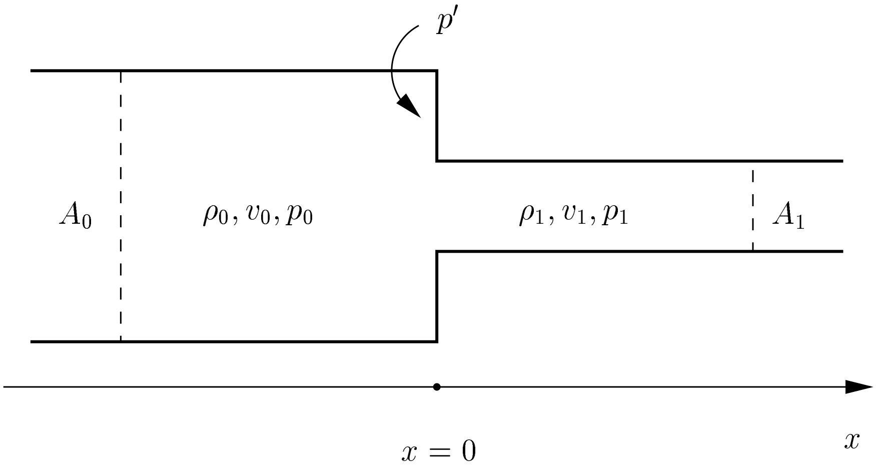

Figure 3: The Riemann problem for the Euler equations in the duct with the sudden change in the cross-section at $x = 0$.

The possible wave configurations, appearing in the solution of the Riemann problem, have been analyzed by Dulov [5] and Yaushev [16].

Note that the equations (5.2) cannot be written in divergence form, exactly as the governing equations for the two-phase flow (2.1). This results in difficulties in determining the jump conditions across the cross-section, where the area of the cross-section has the sudden change. Indeed, the jump conditions are [5]

$$\begin{aligned} [A\rho v] &= 0 \\ \left[A\rho v^2 + Ap\right] &= [A]\, p' \\ [Av(\rho E + p)] &= 0, \end{aligned}$$

where $[\cdot] = (\cdot)_1 - (\cdot)_0$, and p' is the pressure at the ledge, see Fig. 3. The expression for p' has to be determined from some additional considerations. In [5, 16], the authors make different assumptions to this end.

For the solution of the Riemann problem for the two-phase flow equations (2.1), we wish to use the similarities mentioned above. However, the solution of the "direct" Riemann problem will meet the same difficulties as in the case of (5.2). Let us carry out the characteristic analysis of the system (5.2), and find the eigenvalues

$$\lambda_1 = v - c, \quad \lambda_2 = 0, \quad \lambda_3 = v, \quad \lambda_4 = v + c,$$

and the corresponding eigenvectors $\mathbf{r}_i$, $i = 1, \ldots, 4$. The first, third, and fourth characteristic fields are the same as for the Euler equations, and the second one corresponds to the jump in the cross-section. It is obviously linearly degenerate,

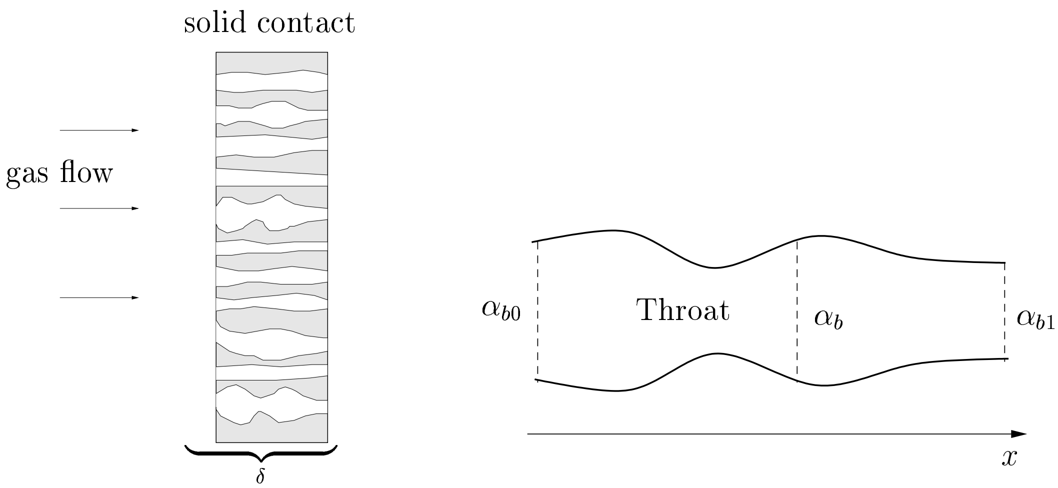

Figure 4: Left: Gas flow through the solid contact. Right: a pore of the variable cross-section.

$\nabla\lambda_2 \cdot \mathbf{r}_2 = 0$, and the Riemann invariants are

$$\begin{aligned} A\rho v &= \text{const} \\ \eta &= \text{const} \\ \mu^2 v^2 + (1-\mu^2)c^2 &= \text{const}, \end{aligned} \tag{5.3}$$

across it. Here η is the isentrope, c is the sound speed, and $\mu^2 = (\gamma-1)/(\gamma+1)$. Note that the relations (5.3) express the conservation of mass, entropy, and Bernoulli's law, respectively, see e.g. Courant and Friedrichs [4].

Observe that the relations (5.3) are very similar to the equations (3.4), expressing the constancy of the Riemann invariants across the solid contact. This gives us reason to consider the solid contact as a porous film of infinitesimal thickness δ, $\delta \to 0$, see Fig. 4. Each pore represents a duct of variable cross section. The solid phase forms the walls of the duct. The values of α_b at the both sides of this porous film are given and equal to α_{b0} and α_{b1}, respectively. Also, the whole gas state is given on the one side of the film. Within the duct, the gas volume fraction α_b changes from α_{b0} to α_{b1} and represents the change of the area of cross-section. The gas flow in the duct is governed by the relations (3.4). Using the similarity between (3.4) and (5.3), we can repeat the classical analysis of [4] to obtain the equality

$$\frac{d\alpha_b}{\alpha_b} = \left(\frac{v^2}{c_b^2} - 1\right)\frac{dv}{v}, \tag{5.4}$$

where now $v = u_b - u_a$ is the gas velocity relative to the velocity of the solid contact, and c_b is the gas sound speed. It is analogous to the well-known relation for the steady, isentropic Euler equations in the duct of variable cross-section, see [4].

We can easily establish several properties of this pore flow. Firstly, we know that the flow is isentropic, see (3.4b). Therefore, *no shocks are allowed in the flow.* For simplicity, let the relative velocity v be positive, $v > 0$. The case of negative v can be considered analogously. Then, from (5.4) we can state that *for increasing α_b the relative speed v increases when $v^2 > c_b^2$ and decreases when $v^2 < c_b^2$.* Using (3.4), we conclude that *in the direction of increasing α_b the gas flow is expanded when it is supersonic, and compressed when it is subsonic.* Finally, the *gas flow relative to the solid contact is superonic(subsonic) at the one side of the solid contact, iff it is also superonic(subsonic) at the other side of it.* To see this, consider the different cases in the proof of Theorem 4.6. It is convenient to represent these results in the following table, where $\uparrow$ denotes increase, and $\downarrow$ decrease.

Supersonic	$\alpha_b \uparrow$	$v \uparrow$	$\rho_b \downarrow$	$c_b \downarrow$
	$\alpha_b \downarrow$	$v \downarrow$	$\rho_b \uparrow$	$c_b \uparrow$
Subsonic	$\alpha_b \uparrow$	$v \downarrow$	$\rho_b \uparrow$	$c_b \uparrow$
	$\alpha_b \downarrow$	$v \uparrow$	$\rho_b \downarrow$	$c_b \downarrow$

Note that the duct can have several throats, see Fig. 4. By the classical theory of Laval nozzle, see e.g. [4], the gas flow can change its type from subsonic to supersonic and vice versa only at the throat. From the property established above, we conclude that this change can occur only an *even* number of times.

To summarize, we have rigorously shown the role of the non-conservative terms on the right hand side of the governing two-phase equations (2.1), which was previously stated by Embid and Baer [6], Bdzil et. al. [3] from physical considerations. Namely, the gas volume fraction measures the *porosity* of the solid phase. Then, *the change in porosity acts as a nozzle which can either accelerate or decelerate the gas flow.*

6 Coinciding waves

As we mentioned previously, the characteristic speeds for the Riemann problem (2.1), (3.3) can coincide with each other. Namely, each of the gas eigenvalues

$$u_b - c_b, \quad u_b, \quad u_b + c_b$$

can coincide with either of solid eigenvalues

$$u_a - c_a, \quad u_a, \quad u_a + c_a.$$

However, the solid parameters do not change across the gas waves, and the gas parameters can change only across the solid contact (and of course across the gas waves), see Section 2. Therefore, the potentially interesting cases arise only when the solid contact u_a coincides with either $u_b \pm c_b$ or u_b. Since the characteristic fields $u_b \pm c_b$ can be either rarefactions or shock waves, and u_b is the contact discontinuity, we will consider these three cases separately.

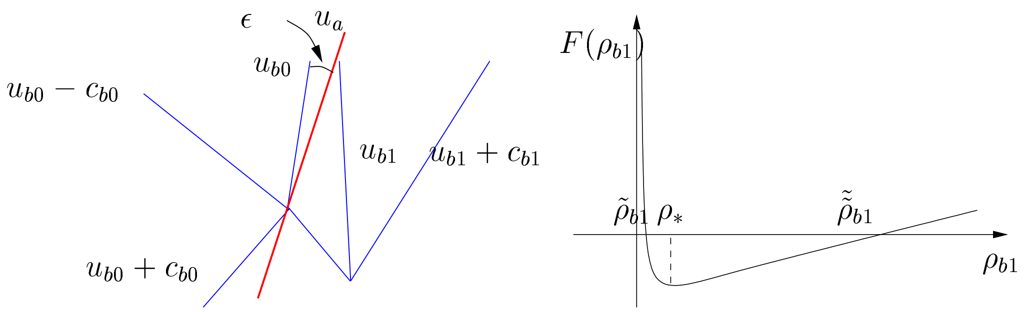

Figure 5: Left: Mutual position of the characteristics when u_{b0} approaches u_a from the left. Right: Roots of (3.6).

6.1 Coinciding contacts

Let us fix α_{b0}, ρ_{b0}, p_{b0} on the left of the solid contact Σ as well as α_{b1} on the right of it. Further let the gas velocity approach u_a from the left, i.e.,

$$u_{b0} + \epsilon = u_a, \qquad \epsilon \to +0, \tag{6.1}$$

see Fig. 5. Note that the characteristic $u_{b0} + c_{b0}$ will impinge on the solid contact from the left.

The state $\mathbf{u}_1$ at the right of the solid contact is determined by the root of (3.6),

$$F(\rho_{b1}) = \frac{1}{2} M_E^2 \left(\frac{\alpha_{b0}}{\alpha_{b1}}\right)^2 \frac{1}{\rho_{b1}^2} + \frac{\gamma_b \eta_b \rho_{b1}^{\gamma_b - 1}}{\gamma_b - 1} - E = 0.$$

By (6.1) and (3.8), we observe that the function F reaches its minimum at the point

$$\rho_*^{\gamma_b+1} = \frac{\alpha_{b0}^2 \rho_{b0}^2}{\alpha_{b1}^2 \gamma_b \eta_b} \epsilon^2 \to 0, \quad \epsilon \to +0.$$

Thus, the root $\rho_{b1} = \tilde{\rho}_{b1}$ becomes infinitely small,

$$\rho_{b1} \to 0, \quad \epsilon \to +0$$

see Fig. 5. Let us show that this root is not admissible. By Theorem 4.6, for the *admissible state* behind the solid contact, the following condition must hold,

$$u_{b1} + c_{b1} > u_a.$$

It states that the characteristic $u_{b1} + c_{b1}$ cannot impinge on the solid contact from the right, cf. Fig. 5. Since $u_{b1} < u_a$, this condition is equivalent to

$$(u_{b1} - u_a)^2 - c_{b1}^2 < 0. \tag{6.2}$$

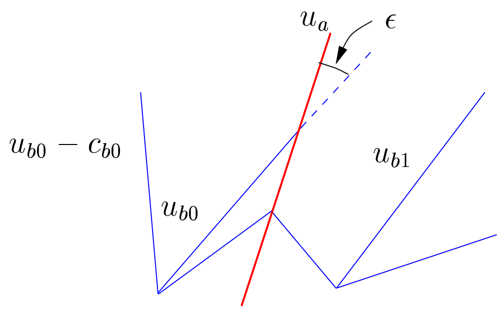

Figure 6: Mutual position of the characteristics when u_{b0} approaches u_a from the right.

Using (3.4e), one has

$$(u_{b1} - u_a)^2 - c_{b1}^2 < 2E - \frac{\gamma_b + 1}{\gamma_b - 1} c_{b1}^2 = 2E - \frac{\gamma_b + 1}{\gamma_b - 1} \eta \gamma_b \rho_{b1}^{\gamma_b - 1} < 0,$$

if ρ_{b1} exceeds some positive constant, i.e.

$$\eta \gamma_b \rho_{b1}^{\gamma_b - 1} > \frac{\gamma_b - 1}{\gamma_b + 1} 2E. \tag{6.3}$$

Therefore, the root $\rho_{b1} \to 0$ gives the non-admissible solution to (3.6), and we can restrict ourselves only to the values of ρ_{b1} which satisfy the condition (6.3).

Now, we will use the fact that the root ρ_{b1} remains finite to determine other variables to the right of the solid contact. By (3.4c), we see that for $\epsilon \to +0$

$$u_{b1} \to u_a.$$

We can rewrite (3.4c) as

$$\frac{(u_{b0} - u_a)^2}{2} + \frac{\gamma_b \eta_b \rho_{b0}^{\gamma_b - 1}}{\gamma_b - 1} = \frac{(u_{b1} - u_a)^2}{2} + \frac{\gamma_b \eta_b \rho_{b1}^{\gamma_b - 1}}{\gamma_b - 1}.$$

Then by (3.4b), for $\epsilon \to +0$

$$\begin{aligned} \rho_{b1} &\to \rho_{b0} \\ p_{b1} &\to p_{b0}. \end{aligned}$$

The situation when u_{b0} approaches u_a from the right, i.e.,

$$u_{b0} + \epsilon = u_a, \qquad \epsilon \to -0.$$

can be handled analogously. Indeed, in this case there are two gas-related characteristics, impinging on the solid contact from the left, so the characteristics $u_{b1} - c_{b1}$ should impinge on it from the right,

$$u_{b1} - c_{b1} < u_a,$$

see Fig. 6. By (3.4c), if $u_{b0} > u_a$ then $u_{b1} > u_a$, so this condition is equivalent to

$$(u_{b1} - u_a)^2 - c_{b1}^2 < 0,$$

which is the same as (6.2), so we can repeat the preceeding analysis. Thus, we have proved the following theorem.

Theorem 6.1. *Let us fix α_{b0}, ρ_{b0}, p_{b0} at the left of the solid contact u_a and α_{b1} at the right of it. Then, as the gas velocity approaches u_a, the gas density and velocity at the right approach the ones at the left,*

$$u_{b0} \to u_a \;\Rightarrow\; \rho_{b1} \to \rho_{b0}, \quad u_{b1} \to u_a, \quad p_{b1} \to p_{b0}.$$

At the limit,

$$u_{b0} = u_a \;\Rightarrow\; \rho_{b1} = \rho_{b0}, \quad u_{b1} = u_a, \quad p_{b1} = p_{b0}.$$

We can easily show that in case of coinciding contacts the solid contact remains an evolutionary discontinuity. Indeed, now we have 4 gas-related incoming or coinciding waves, and the formulation of the "inverse" problem can be seen as follows,

$$\underbrace{\rho_{a0}, u_{a0}, p_{a0}, \rho_{a1}, \alpha_{a0}, \alpha_{a1},}_{\substack{\text{from 6 incoming or coinciding} \\ \text{solid characteristics}}} \quad \underbrace{\rho_{b0}, u_{b0}, p_{b0}, \rho_{b1}}_{\substack{\text{from 4 incoming or coin-} \\ \text{ciding gas characteristics}}} \quad \underbrace{u_{a1}, p_{a1},}_{\substack{\text{for 2 outcoming} \\ \text{solid characteristics}}} \quad \underbrace{u_{b1}, p_{b1},}_{\substack{\text{for 2 outcoming} \\ \text{gas characteristics}}}$$

cf. Remark 4.5.

6.2 Sonic state attached to the solid contact

Let us consider the critical case when

$$(u_b - u_a)^2 \to c_b^2 \tag{6.4}$$

from either side of the solid contact Σ. From (2.5) we know that then the eigenvectors of (3.2) become linearly degenerate. Consequently, we cannot write the system of governing equations (3.1) in characteristic form. Therefore, the results of Section 4, in particular Theorem 4.4, do not hold anymore. Theorem 4.12 cannot even be formulated.

Using the gas dynamics analogy, it is easy to see that an infinitesimal change in the state $\mathbf{u}_0$ to the left of the solid contact Σ leads to a jump in $\mathbf{u}_1$ to the right of it. With the results of Section 5 the reason for this behaviour becomes evident. The difference of $\alpha_{b0} - \alpha_{b1}$ determines if each pore represents a converging or diverging nozzle, see Fig. 4 . This flow is governed by (5.4). Consider the flow such the condition (6.4) holds at the cross-section α_{b0}, i.e. at the state $\mathbf{u}_0$ to the left of Σ. Then, the relative gas flow there is almost sonic,

$$\mathrm{M}_0 = \frac{u_{b0} - u_a}{c_{b0}} = 1 + \epsilon, \qquad \epsilon \to \pm 0.$$

Depending on the sign of ϵ and on the difference $\alpha_{b1} - \alpha_{b0}$, the gas flow in the pore either accelerates and expands, or decelerates and compresses, leading to the very different states $\mathbf{u}_1$ to the right of Σ. Thus, such a sonic configuration is not stable.

We can also give an interpretation to the case when the equation (3.11) has no roots. As it was mentioned in Section 3, the equation (3.11) has no roots when α_{b1} becomes sufficiently small, cf. (3.10). According to the results of Section 5, the change of the gas parameters to the right of the solid contact is determined whether the gas relative speed $u_b - u_a$ is subsonic or supersonic. When it is subsonic, then the gas flow accelerates and expands, so the sound speed and the relative Mach number $\mathrm{M} = |u_{b1} - u_a|/c_{b1}$ decrease. As soon as the gas volume fraction falls below its critical value, where $\mathrm{M} = 1$, a shock intervenes and the isentropic flow does not exist anymore. On the other hand, when the gas relative flow is supersonic, the gas velocity decreases, and the sound speed and the relative Mach number increase. Again, for the gas volume fraction below its critical value, the isentropic flow does not exist. Geometrically, we can illustrate the possible scenarios by considering the different cases of the proof of Theorem 4.6.

I.A. 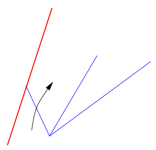 One root: $u_{b1} - c_{b1} = u_a$, no roots: $u_{b1} - c_{b1} > u_a$

I.B. 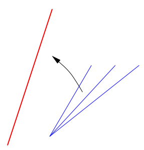 One root: $u_{b1} - c_{b1} = u_a$, no roots: $u_{b1} - c_{b1} < u_a$

II.A. 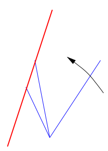 One root: $u_{b1} + c_{b1} = u_a$, no roots: $u_{b1} - c_{b1} < u_a$

II.B. 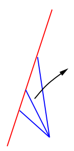 One root: $u_{b1} + c_{b1} = u_a$, no roots: $u_{b1} + c_{b1} > u_a$

It is an easy matter to check that the solid contact can lie *inside* of the gas rarefaction only in the trivial case when $\mathbf{u}_0 = \mathbf{u}_1$, $\mathbf{u}$ is given by (3.2). Then in particular $\alpha_{b0} = \alpha_{b1}$, so that the phases are decoupled. For simplicity, consider the gas 1-rarefaction (the case of 3-rarefaction can be done analogously). In the rarefaction wave, $u_b - c_b$ varies monotonically across the wave, so that the following equality should hold true,

$$u_{b0} - c_{b0} = u_a = u_{b0} + c_{b0}.$$

Using this in (3.4), we get

$$\mathbf{u}_0 = \mathbf{u}_1.$$

6.3 Shock vs. solid contact

Finally, let us describe the behaviour of the solution, when the (admissible) gas shock wave approaches the solid contact. For simplicity, we consider the shock at the left of the solid contact, i.e., $s \to u_a$, $s < u_a$, see Fig. 7.

Across the shock, the Rankine–Hugoniot conditions hold, and across the solid contact — the relations (3.4). Combining them, we get

$$\rho_b(u_b - s) = \rho_{b0}(u_{b0} - s) \to \rho_{b1}\frac{\alpha_{b1}}{\alpha_{b0}}(u_{b1} - u_{b0}) = \frac{M}{\alpha_{b0}} =: M_1 \tag{6.5a}$$

$$\rho_b(u_b - s)^2 + p_b = \rho_{b0}(u_{b0} - s)^2 + p_{b0} \to \frac{1}{\alpha_{a1}}(P - \alpha_{a0}p_{a0}) =: P_1 \tag{6.5b}$$

$$\frac{(u_b - s)^2}{2} + \frac{c_b^2}{\gamma_b - 1} = \frac{(u_{b0} - s)^2}{2} + \frac{c_{b0}^2}{\gamma_b - 1} \to \frac{(u_{b1} - u_a)^2}{2} + \frac{c_{b1}^2}{\gamma_b - 1} = E \tag{6.5c}$$

as $s \to u_a$. Multiply (6.5c) by $2\rho_b$, and substract the result from (6.5b). Then

$$p_b\frac{\gamma_b + 1}{1 - \gamma_b} - \frac{2\gamma_b\pi_b}{\gamma_b - 1} \to P_1 - 2\rho_b E. \tag{6.6}$$

From (6.5a) and (6.5b)

$$p_b \to P_1 - \frac{M_1^2}{\rho_b}.$$

Substituting this into (6.6), we get the following relation for ρ_b,

$$(P_1 - \frac{M_1^2}{\rho_b})\frac{\gamma_b + 1}{1 - \gamma_b} - \frac{2\gamma_b\pi_b}{\gamma_b - 1} \to P_1 - 2\rho_b E.$$

In the limit it reveals the quadratic equation for ρ_b,

$$(P_1 - \frac{M_1^2}{\rho_b})\frac{\gamma_b + 1}{1 - \gamma_b} - \frac{2\gamma_b\pi_b}{\gamma_b - 1} = P_1 - 2\rho_b E,$$

$\rho_b \neq 0$. This equation has two roots. One of them is always ρ_{b0}, and corresponds to the state $\mathbf{u} \equiv \mathbf{u}_0$. The other is necessarily admissible, since we consider the

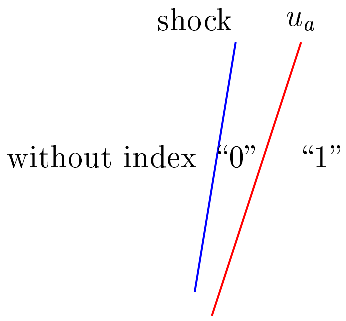

Figure 7: Gas shock approaches the solid contact from the left.

admissible shock wave. Using this root, we can find the state behind the shock

$$\begin{aligned} u_b &= \frac{M_1^2}{\rho_b} + s \\ p_b &= P_1 - \frac{M_1^2}{\rho_b}. \end{aligned} \tag{6.7}$$

Thus, we see that the state behind the shock approaches some finite state which is given by (6.7), as the shock approaches the solid contact.

7 Weak solution

As we have mentioned before, one cannot define a weak solution to the system (3.1) in a usual manner, as it is done for the system of conservation laws. The reason is that the system (3.1) cannot be written in divergence form. For the Riemann problem (3.1)-(3.3), however, this difficulty appears only along one line, namely the solid contact, where the volume fraction α_a is discontinuous. In the rest of domain, the volume fraction is constant and equal to its left or right value,

$$\alpha(x,t) = \begin{cases} \alpha_{aL}, & (x,t) \text{ lies to the left of solid contact} \\ \alpha_{aR}, & (x,t) \text{ lies to the right of it.} \end{cases}$$

Therefore, everywhere away from the solid contact the system (2.1) reduces to the system of *conservation laws*

$$\mathbf{u}_t + \mathbf{f}(\mathbf{u})_x = 0, \tag{7.1}$$

where

$$\mathbf{u} = \begin{bmatrix} \rho_a \\ \rho_a u_a \\ \rho_a E_a \\ \rho_b \\ \rho_b u_b \\ \rho_b E_b \end{bmatrix}, \quad \mathbf{f}(\mathbf{u}) = \begin{bmatrix} \rho_a u_a \\ \rho_a u_a^2 + p_a \\ u_a(\rho_a E_a + p_a) \\ \rho_b u_b \\ \rho_b u_b^2 + p_b \\ u_b(\rho_b E_b + p_b) \end{bmatrix}. \tag{7.2}$$

Note that this system is just the two sets of uncoupled Euler equations for the phase a and b. For the system (7.1), we can define a weak solution in the usual manner, see Definition 7.2 below.

From the other hand, across the solid contact, the relations (3.4) hold true. Our main idea is to find a system of equations, which give the relations (3.4) as a relations across the solid contact. In other words, we reverse the usual process of obtaining the Rankine–Hugoniot conditions for the system of conservation laws. There, one starts with a system of equations and gets the relations across a discontinuity. Here, we start from the relations across the discontinuity and wish to find the system of equations.

Let us rewrite the relations (3.4) in the form, which is reminiscent of the Rankine–Hugoniot conditions $s[\mathbf{u}] = [\mathbf{f}]$. The mass balance (3.4c) is

$$u_a(\alpha_{b1}\rho_{b1} - \alpha_{b0}\rho_{b0}) = \alpha_{b1}\rho_{b1}u_{b1} - \alpha_{b0}\rho_{b0}u_{b0}. \tag{7.3}$$

The momentum equation (3.4d) can be rewritten as

$$P_0 + Mu_{b0} = P_1 + Mu_{b1}, \tag{7.4}$$

where $P_i = \alpha_{ai}p_{ai} + \alpha_{bi}p_{bi}$, $i = 0, 1$. This is equivalent to

$$u_a(\alpha_{b1}\rho_{b1}u_{b1} - \alpha_{b0}\rho_{b0}u_{b0}) = (P_1 + \alpha_{b1}\rho_{b1}u_{b1}^2) - (P_0 + \alpha_{b0}\rho_{b0}u_{b0}^2). \tag{7.5}$$

Multiply the energy equation (3.4e) by M, and add it to (7.4), multiplied by u_a. The result can be rewritten as

$$\begin{aligned} u_a\left[(\alpha_{b1}\rho_{b1}E_{b1} - \alpha_{a1}p_{a1}) - (\alpha_{b0}\rho_{b0}E_{b0} - \alpha_{a0}p_{a0})\right] = \\ \alpha_{b1}u_{b1}(\rho_{b1}E_{b1} + p_{b1}) - \alpha_{b0}u_{b0}(\rho_{b0}E_{b0} + p_{b0}). \end{aligned} \tag{7.6}$$

Finally, near the solid contact

$$\begin{aligned} u_a &= \text{const} \\ \eta_b &= \text{const}. \end{aligned} \tag{7.7}$$

The relations (7.3), (7.3), and (7.6) may be written in the vector form

$$u_a\left(\tilde{\mathbf{U}}_1 - \tilde{\mathbf{U}}_0\right) = \tilde{\mathbf{F}}_1 - \tilde{\mathbf{F}}_0, \tag{7.8}$$

where

$$\tilde{\mathbf{U}} = \begin{bmatrix} \alpha_b\rho_b \\ \alpha_b\rho_b u_b \\ \alpha_b\rho_b E_b - \alpha_a p_a \end{bmatrix}, \quad \tilde{\mathbf{F}} = \begin{bmatrix} \alpha_b\rho_b u_b \\ \alpha_b\rho_b u_b^2 + P_i \\ \alpha_b u_b(\rho_b E_b + p_b) \end{bmatrix},$$

$P_i = \alpha_{ai}p_{ai} + \alpha_{bi}p_{bi}$, $i = 0, 1$. The equations (7.8) can be interpreted as the Rankine–Hugoniot relations across the solid contact for the system

$$\frac{\partial\tilde{\mathbf{U}}(\mathbf{u};\alpha_a)}{\partial t} + \frac{\partial\tilde{\mathbf{F}}(\mathbf{u};\alpha_a)}{\partial x} = 0. \tag{7.9}$$

Note that (7.9) is the *undetermined* system for finding all seven unknowns α_a, ρ_k, u_k, p_k, $k = a, b$. This is not surprising since we have started with the relations (3.4), which also do not give the values of all unknowns on the both sides of the solid contact. In addition to them, we have to prescribe the values of some parameters, see Section 3 for details.

Let us show that for the Riemann problem (2.1) with the Riemann initial data of the form (3.3), the original system (2.1) reduces to the *conservative* system, such that

- A part of this system is equivalent to the system (7.9) and
- The Rankine–Hugoniot conditions for this system across the solid contact are equivalent to the relations (3.4)

(7.10)

near the solid contact. We will investigate, to which system does the original system (2.1) reduce under the conditions (7.7). Using $u_a = \text{const}$ in (2.1), we get

$$\frac{\partial \alpha_a}{\partial t} + \frac{\partial u_a \alpha_a}{\partial x} = 0 \tag{7.11a}$$

$$\frac{\partial \alpha_a \rho_a}{\partial t} + \frac{\partial \alpha_a \rho_a u_a}{\partial x} = 0 \tag{7.11b}$$

$$(p_a - p_b)\frac{\partial \alpha_a}{\partial x} + \alpha_a \frac{\partial p_a}{\partial x} = 0 \tag{7.11c}$$

$$\frac{\partial p_a}{\partial t} + \frac{\partial u_a p_a}{\partial x} = 0 \tag{7.11d}$$

$$\frac{\partial \alpha_b \rho_b}{\partial t} + \frac{\partial \alpha_b \rho_b u_b}{\partial x} = 0 \tag{7.11e}$$

$$\frac{\partial \alpha_b \rho_b u_b}{\partial t} + \frac{\partial (\alpha_b \rho_b u_b^2 + \alpha_b p_b)}{\partial x} = -p_b \frac{\partial \alpha_a}{\partial x} \tag{7.11f}$$

$$\frac{\partial \alpha_b \rho_b E_b}{\partial t} + \frac{\partial \alpha_b u_b (\rho_b E_b + p_b)}{\partial x} = -p_b u_a \frac{\partial \alpha_a}{\partial x}. \tag{7.11g}$$

Using (7.11c), (7.11d) in (7.11f) and (7.11g), we obtain

$$\frac{\partial \alpha_b \rho_b u_b}{\partial t} + \frac{\partial (\alpha_b \rho_b u_b^2 + \alpha_a p_a + \alpha_b p_b)}{\partial x} = 0 \tag{7.12}$$

$$\frac{\partial (\alpha_b \rho_b E_b - \alpha_a p_a)}{\partial t} + \frac{\partial \alpha_b u_b (\rho_b E_b + p_b)}{\partial x} = 0. \tag{7.13}$$

Also, the equation (7.11g) is equivalent to

$$\frac{\partial \eta_b}{\partial t} + u_b \frac{\partial \eta_b}{\partial x} = 0. \tag{7.14}$$

It is an easy matter to check that the system

$$\frac{\partial \alpha_a}{\partial t} + \frac{\partial u_a \alpha_a}{\partial x} = 0 \tag{7.15a}$$

$$\frac{\partial \alpha_a \rho_a}{\partial t} + \frac{\partial \alpha_a \rho_a u_a}{\partial x} = 0 \tag{7.15b}$$

$$\frac{\partial p_a}{\partial t} + \frac{\partial u_a p_a}{\partial x} = 0 \tag{7.15c}$$

$$\frac{\partial \alpha_b \rho_b}{\partial t} + \frac{\partial \alpha_b \rho_b u_b}{\partial x} = 0 \tag{7.15d}$$

$$\frac{\partial \alpha_b \rho_b u_b}{\partial t} + \frac{\partial (\alpha_b \rho_b u_b^2 + \alpha_a p_a + \alpha_b p_b)}{\partial x} = 0 \tag{7.15e}$$

$$\frac{\partial (\alpha_b \rho_b E_b - \alpha_a p_a)}{\partial t} + \frac{\partial \alpha_b u_b (\rho_b E_b + p_b)}{\partial x} = 0 \tag{7.15f}$$

$$\frac{\partial \eta_b}{\partial t} + u_b \frac{\partial \eta_b}{\partial x} = 0 \tag{7.15g}$$

is equivalent to the system (7.11) when u_a = const. Posing also the second condition of (7.7), η_b = const, the last equations of (7.11) and (7.15) drop off, that is, (7.11g) and (7.15g). Thus, the original system (2.1) is equivalent to the system

$$\frac{\partial \mathbf{U}}{\partial t} + \frac{\partial \mathbf{F}(\mathbf{U}, u_a)}{\partial x} = 0. \tag{7.16}$$

under the conditions (7.7) with

$$\mathbf{U} = \begin{bmatrix} \alpha_a \\ \alpha_a \rho_a \\ p_a \\ \alpha_b \rho_b \\ \alpha_b \rho_b u_b \\ \alpha_b \rho_b E_b - \alpha_a p_a \end{bmatrix}, \quad \mathbf{F}(\mathbf{U}, u_a) = \begin{bmatrix} \alpha_a u_a \\ \alpha_a \rho_a u_a \\ p_a u_a \\ \alpha_b \rho_b u_b \\ \alpha_b \rho_b u_b^2 + \alpha_a p_a + \alpha_b p_b \\ \alpha_b u_b (\rho_b E_b + p_b) \end{bmatrix}. \tag{7.17}$$

We see that the both conditions (7.10) are fulfilled. Indeed, the system (7.9) is just the last three equations of (7.16). Across the solid contact, which is a discontinuity propagating with speed u_a, the Rankine–Hugoniot conditions coincide with (3.4).

Next, let us define a weak solution to the Riemann problem for a conservation law

$$\mathbf{u}_t + \mathbf{f}(\mathbf{u})_x = 0, \qquad \mathbf{u}(x, 0) = \begin{cases} \mathbf{u}_L, & x \leq 0 \\ \mathbf{u}_R, & x > 0. \end{cases} \tag{7.18}$$

As usual, we consider the self-similar solutions, i.e.,

$$\mathbf{u}(x, t) = \mathbf{v}(\xi), \qquad \xi = \frac{x}{t}.$$

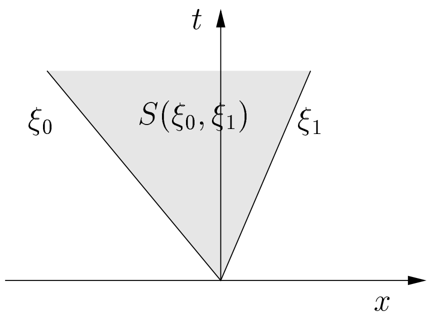

Figure 8: A test function $\phi \equiv 0$ outside of $S(\xi_0, \xi_1)$ and on the rays ξ_0, ξ_1.

Then, the Riemann problem (7.18) is equivalent to

$$-\mathbf{v}_\xi \cdot \xi + \mathbf{f}(\mathbf{v})_\xi = 0, \quad \mathbf{v}(-\infty) = \mathbf{v}_L, \quad \mathbf{v}(\infty) = \mathbf{v}_R. \tag{7.19}$$

Let us suppose for the moment, that $\mathbf{v}$ is a classical solution of (7.19). Denote by $S(\xi_0, \xi_1)$ the sector, bounded by the rays ξ_0 and ξ_1. Also, let $C_0^1(]\xi_0, \xi_1[)$ be the class of all test functions ϕ which vanish outside of the open interval $]\xi_0, \xi_1[$, see Fig. 8. We multiply (7.19) by ϕ and integrate over all ξ,

$$\int_{-\infty}^{\infty} (-\mathbf{v}_\xi \cdot \xi + \mathbf{f}(\mathbf{v})_\xi)\phi(\xi)\, d\xi = \int_{\xi_0}^{\xi_1} (-\mathbf{v}_\xi \cdot \xi + \mathbf{f}(\mathbf{v})_\xi)\phi(\xi)\, d\xi.$$

Integrating by parts gives

$$\begin{aligned} \int_{\xi_0}^{\xi_1} (-\mathbf{v}_\xi \cdot \xi + \mathbf{f}(\mathbf{v})_\xi)\phi\, d\xi &= (-\xi\phi\mathbf{v} + \phi\mathbf{f}(\mathbf{v}))\Big|_{\xi_0}^{\xi_1} + \int_{\xi_0}^{\xi_1} (\mathbf{v}(\phi \cdot \xi)_\xi - \mathbf{f}(\mathbf{v})\phi_\xi)\, d\xi \\ &= \int_{\xi_0}^{\xi_1} (\mathbf{v}(\phi \cdot \xi)_\xi - \mathbf{f}(\mathbf{v})\phi_\xi)\, d\xi = 0. \end{aligned} \tag{7.20}$$

Thus, if $\mathbf{v}$ is a classical solution of (7.19), then (7.20) holds true for all $\phi \in C_0^1(]\xi_0, \xi_1[)$. However, $\mathbf{v}$ does not need to be differentiable anymore. This gives rise to the following definition.

Definition 7.1. *A bounded measurable function* $\mathbf{v} = \mathbf{v}(\xi)$ *is called a weak solution to the Riemann problem* (7.19) *if* $\mathbf{v}$ *satisfies* (7.20) *for all* $\phi \in C_0^1(]\xi_0, \xi_1[)$.

Let us check, if we can get the Rankine–Hugoniot conditions across a discontinuity from this definition. Consider a discontinuity s and a sector $S(s_0, s_1)$ such that $s \in S(s_0, s_1)$ and s is the only discontinuity there. Let $\phi \in C_0^1(]s_0, s_1[)$ be some test function. The weak solution of (7.19) in $S(s_0, s_1)$ is defined by

$$\int_{s_0}^{s_1} (\mathbf{v}(\phi \cdot \xi)_\xi - \mathbf{f}(\mathbf{v})\phi_\xi)\, d\xi = 0.$$

Splitting the integral and integrating by parts,

$$\begin{aligned}
&\int_{s_0}^{s_1} (\mathbf{v}(\phi \cdot \xi)_\xi - \mathbf{f}(\mathbf{v})\phi_\xi)\, d\xi \\
&\qquad = \int_{s_0}^{s} (\mathbf{v}(\phi \cdot \xi)_\xi - \mathbf{f}(\mathbf{v})\phi_\xi)\, d\xi + \int_{s}^{s_1} (\mathbf{v}(\phi \cdot \xi)_\xi - \mathbf{f}(\mathbf{v})\phi_\xi)\, d\xi \\
&\qquad = (-\xi\phi\mathbf{v} + \phi\mathbf{f}(\mathbf{v}))\Big|_{\mathbf{s}_0}^{s} + \int_{s_0}^{s} (-\mathbf{v}_\xi \cdot \xi + \mathbf{f}(\mathbf{v})_\xi)\phi\, d\xi \\
&\qquad\quad + (-\xi\phi\mathbf{v} + \phi\mathbf{f}(\mathbf{v}))\Big|_{s}^{s_1} + \int_{s}^{s_1} (-\mathbf{v}_\xi \cdot \xi + \mathbf{f}(\mathbf{v})_\xi)\phi\, d\xi \\
&\qquad = \phi(s)s(\mathbf{v}_l - \mathbf{v}_r) + \phi(s)(\mathbf{f}(\mathbf{v}_r) - \mathbf{f}(\mathbf{v}_l)) = 0, \qquad (7.21)
\end{aligned}$$

where $\mathbf{v}_l = \mathbf{v}(s-0)$ and $\mathbf{v}_r = \mathbf{v}(s+0)$. Dividing (7.21) by $\phi(s) \neq 0$, we obtain the usual Rankine–Hugoniot relations across s.

Now, using Definition 7.1, we can define a weak solution to the Riemann problem for the *non-conservative* system (2.1). We will utilize the above established fact that everywhere locally this non-conservative system is equivalent to the conservative one, either (7.1) or (7.16).

Definition 7.2. *Consider a sector $S(\xi_0, \xi_1)$, such that the solid contact lies in it, and assume that the solid contact is the only surface of discontiuity in $S(\xi_0, \xi_1)$. Also consider the Riemann initial data*

$$\begin{cases} \mathbf{w}(-\infty) & = (\alpha_a, \rho_a u_a, E_a, \rho_b, \rho_b u_b, E_b)_L^T \\ \mathbf{w}(+\infty) & = (\alpha_a, \rho_a u_a, E_a, \rho_b, \rho_b u_b, E_b)_R^T \end{cases} \qquad (7.22)$$

Then, a function $\mathbf{w} = \mathbf{w}(\xi) \in L^\infty_{loc}(\mathbb{R})$ is called a weak solution of the Riemann problem (2.1)-(7.22), if for any small $\epsilon > 0$

1. *To the left of $S(\xi_0, \xi_1)$, i.e., $\xi \in [-\infty, \xi_0]$, $\mathbf{w} = \mathbf{w}(\mathbf{v}, \alpha_L)$, where $\mathbf{v} = \mathbf{v}(\xi)$ is a weak solution of (7.1),*

$$\int_{-\infty}^{\xi_0} (\mathbf{v}(\phi \cdot \xi)_\xi - \mathbf{f}(\mathbf{v})\phi_\xi)\, d\xi = 0, \qquad \phi \in C_0^1(]-\infty, \xi_0 + \epsilon[),$$

   $\mathbf{v}(\xi) = \mathbf{u}(x,t)$*, and* $\mathbf{u}$, $\mathbf{f}(\mathbf{u})$ *are given by (7.2).*

2. *To the right of $S(\xi_0, \xi_1)$, i.e., $\xi \in [\xi_1, \infty]$, $\mathbf{w} = \mathbf{w}(\mathbf{v}, \alpha_R)$, where $\mathbf{v} = \mathbf{v}(\xi)$ is a weak solution of (7.1),*

$$\int_{\xi_1}^{\infty} (\mathbf{v}(\phi \cdot \xi)_\xi - \mathbf{f}(\mathbf{v})\phi_\xi)\, d\xi = 0, \qquad \phi \in C_0^1(]\xi_1 - \epsilon, \infty[),$$

   $\mathbf{v}(\xi) = \mathbf{u}(x,t)$*, and* $\mathbf{u}$, $\mathbf{f}(\mathbf{u})$ *are given by (7.2).*

3. *Inside of* $S(\xi_0, \xi_1)$, *i.e.,* $\xi \in [\xi_0, \xi_1]$, $\mathbf{w} = \mathbf{w}(\mathbf{V}, u_a(\xi_0))$, *where* $\mathbf{V} = \mathbf{V}(\xi)$ *is a weak solution of* (7.16),

$$\int_{\xi_0}^{\xi_1} (\mathbf{V}(\phi \cdot \xi)_\xi - \mathbf{F}(\mathbf{V}, u_a)\phi_\xi)\, d\xi = 0, \qquad \phi \in C_0^1(]\xi_0 - \epsilon, \xi_1 + \epsilon[),$$

$\mathbf{V}(\xi) = \mathbf{U}(x, t)$, *and* $\mathbf{U}$, $\mathbf{F}(\mathbf{U}, u_a)$ *are given by* (7.17).

Remark 7.3. Note that in the sector $S(\xi_0 - \epsilon, \xi_0 + \epsilon)$, the definitions 1) and 3) coincide, and in the sector $S(\xi_1 - \epsilon, \xi_1 + \epsilon)$, the definitions 2) and 3) coincide.

8 Test cases

As we have seen in Section 2, the system two-phase flow equations (2.1) consists of the two sets of the Euler equations for the both phases, coupled with the non-conservative terms. Therefore, a "good" numerical scheme for the equations (2.1) should be necessarily "good" for the Euler equations. The notion "good" includes the well-known properties, like convergence to the entropy solution, reasonable accuracy, robustness etc. For the Euler equations, one has a number of test cases, intended to check these properties for each particular scheme. An excellent reference is Toro [15].

However, for the two-phase problems, there exists only a small number of test cases, and usually they incorporate several physical effects, specific material properties, and external forces. All these makes it difficult to compare the numerical methods for the two-phase flows.

Here, we propose a number of test cases for the BN model, using the exact solution to the Riemann problem, which was obtained in Section 3. The tests are aimed at the investigation of some specifically two-phase phenomena, which do not have a counterpart in one-phase flows. In particular, a number of tests is designed to assess the behaviour of numerical methods for the Riemann problem with almost coinciding wave speeds. The exact solutions were found by running the package CONSTRUCT, which is freely available at

`http://www.uni-magdeburg.de/andriano/CONSTRUCT`

The data for the following test problems can be also downloaded from the above address.

In Section 5 we have shown that the system of the two-phase flow equations (2.1) reduces to the system of the Euler equations in the duct of variable cross section (5.2), if we set

$$\rho_a \equiv \text{const}, \qquad u_a \equiv 0, \qquad p_a \equiv \text{const}.$$

Thus, under these conditions and if we consider only gas waves in the solution of the Riemann problem, we can use CONSTRUCT for the system (5.2), too. Here, we propose only one test case for the system (5.2). However, one can easily build other exact solutions with CONSTRUCT.

Recently, we have proposed a numerical method for compressible multiphase flows [1]. In what follows, it will be referred to as VFRoe, stands for *Volumes Finis Roe* in French. As it is clear from the name, it employs the features of both Roe's and finite volume methods. At each cell boundary, one solves the linearized Riemann problem as in the Roe's method. Then, we calculate the numerical flux function as the physical flux in the intermediate state of the solution of the Riemann problem. For the non-conservative terms, we use some physically motivated discretization, see [1] for details. In [1], we show the robustness and accuracy of the method on several numerical examples.

Below, we compare the numerical results of VFRoe with the exact solutions to the Riemann problems for the Euler equations in the duct of variable cross section, and for the BN model of two-phase flows. To see clearly the effects of VFRoe discretization, we present here the numerical results of the first order accuracy. The extension to the second order is described in [1]. We have always used 300 mesh cells in the calculations below. For simplicity, we have used the ideal gas EOS, i.e., $\gamma_k = 1.4, \pi_k = 0$ in (2.2), $k = a, b$. The initial position of the discontinuity is always 0.5.

8.1 Euler equations in the duct of variable cross section

Consider the following Riemann problem

A_L	ρ_L	v_L	p_l	A_R	ρ_R	v_R	p_R
0.6	0.96	1.0833	2.8333	0.7	1.7741	1.1187	4.0

The solution consists of the 1-shock wave, travelling to the left, stationary wave corresponding to the jump in the cross-section, contact wave, and the 3-rarefaction. The comparison of the numerical solution with the exact one is presented in Fig. 9.

8.2 Test cases for the BN model

Test 1: Single solid contact Consider the following Riemann problem for the BN model

Phase k	α_{kL}	ρ_{kL}	u_{kL}	p_{kL}	a_{kR}	ρ_{kR}	u_{kR}	p_{kR}
a	0.8	2	0.3	5	0.3	2	0.3	12.8567
b	0.2	1	2	1	0.7	0.1941	2.8011	0.10

Its solution consists of the single solid contact, propagating with the velocity 0.3. The numerical results are presented in Fig. 10. In this test, the jump of the volume fraction $\alpha_{aR} - \alpha_{aL} = 0.5$.

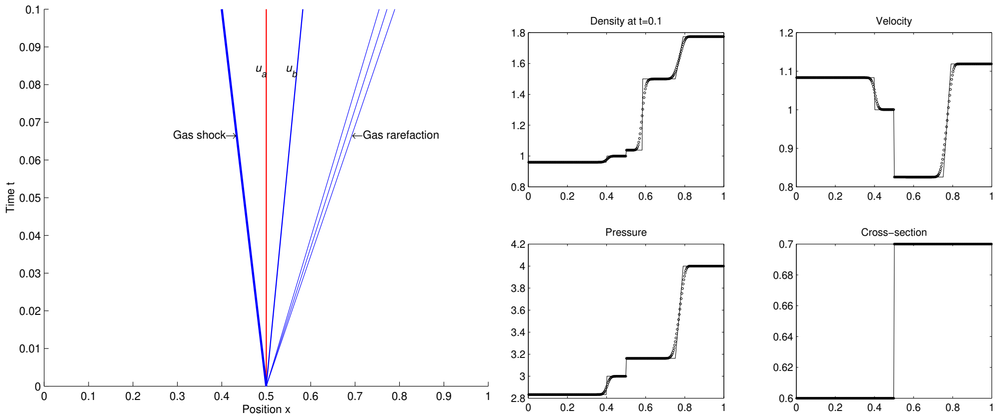

Figure 9: The Riemann problem for the Euler equations in the duct of variable cross section.

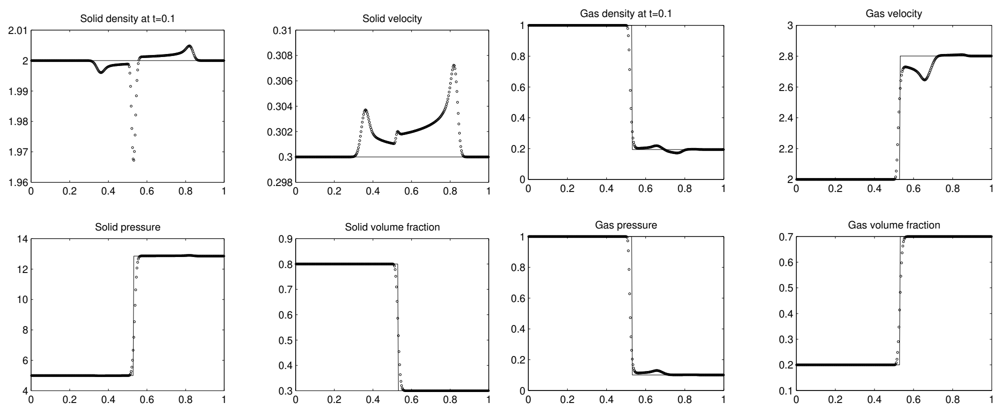

Figure 10: The numerical results for Test 1.

Test 2: Coinciding shocks and rarefactions A particular issue on the Riemann problem for the equations (2.1) is that several waves can coincide with each other. However, the gas parameters do not change across the solid waves (except of the solid contact) and vice versa, see Section 2. Thus, the numerical solution across these waves should be independent of the presence of the wave of the other phase. If we take the initial data as follows

Phase k	α_{kL}	ρ_{kL}	u_{kL}	p_{kL}	a_{kR}	ρ_{kR}	u_{kR}	p_{kR}
a	0.1	0.2068	1.4166	0.0416	0.2	2.2263	0.9366	6.0
b	0.9	0.5806	1.5833	1.375	0.8	0.4890	-0.70138	0.986

then the Riemann solution consists of two coinciding 1-shock waves for the gas and solid, and the gas 3-shock inside of the solid 3-rarefaction. The structure

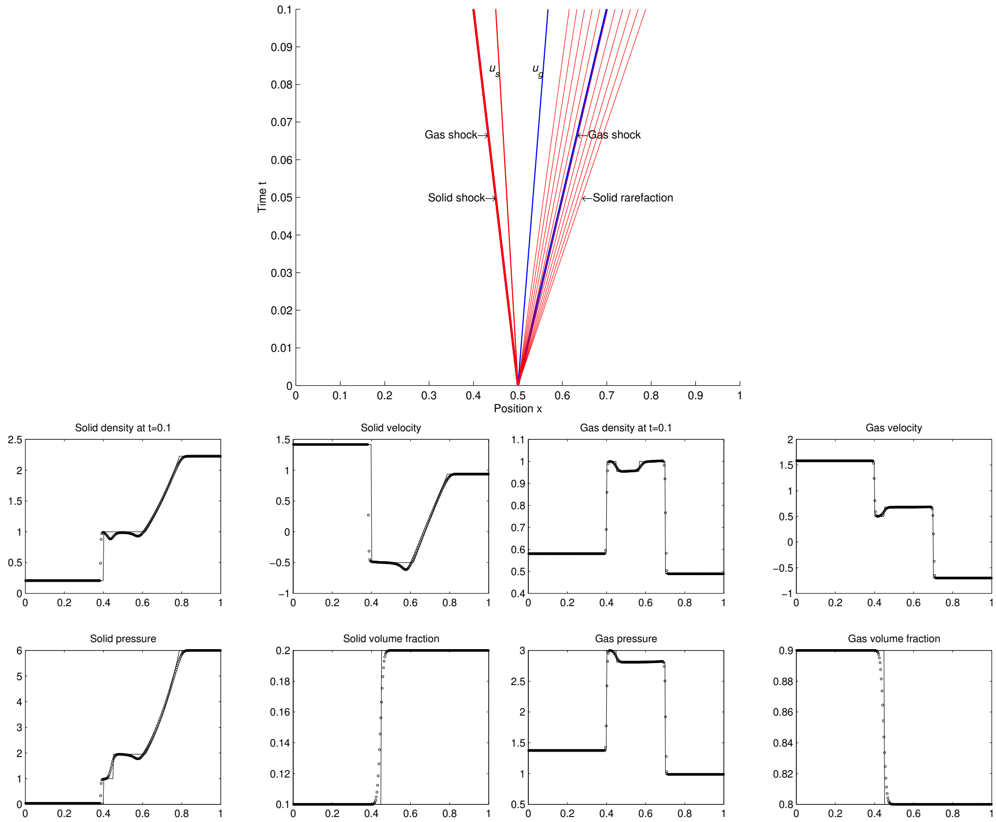

Figure 11: The Riemann problem for Test 2.

of the Riemann problem and the numerical results for this test are presented in Fig. 11.

Test 3: Coinciding contacts When the solid and gas contacts approach each other, both u_a and p_b are almost constant there, see Section 6. Therefore, the non-conservative terms (2.3)

$$p_b \frac{\partial \alpha_a}{\partial x} \approx \frac{\partial p_b \alpha_a}{\partial x}, \qquad p_b u_a \frac{\partial \alpha_a}{\partial x} \approx \frac{\partial p_b u_a \alpha_a}{\partial x}$$

near the solid contact. Thus, this test should not pose serious difficulties. This configuration occurs if we take the following initial data

Phase k	α_{kL}	ρ_{kL}	u_{kL}	p_{kL}	a_{kR}	ρ_{kR}	u_{kR}	p_{kR}
a	0.1	0.9123	1.6305	1.5666	0.9	0.8592	-0.0129	1.1675
b	0.9	2.6718	-0.050	1.5	0.1	1.3359	0.5438	1.5

The structure of the Riemann problem and the numerical results for this test are presented in Fig. 12.

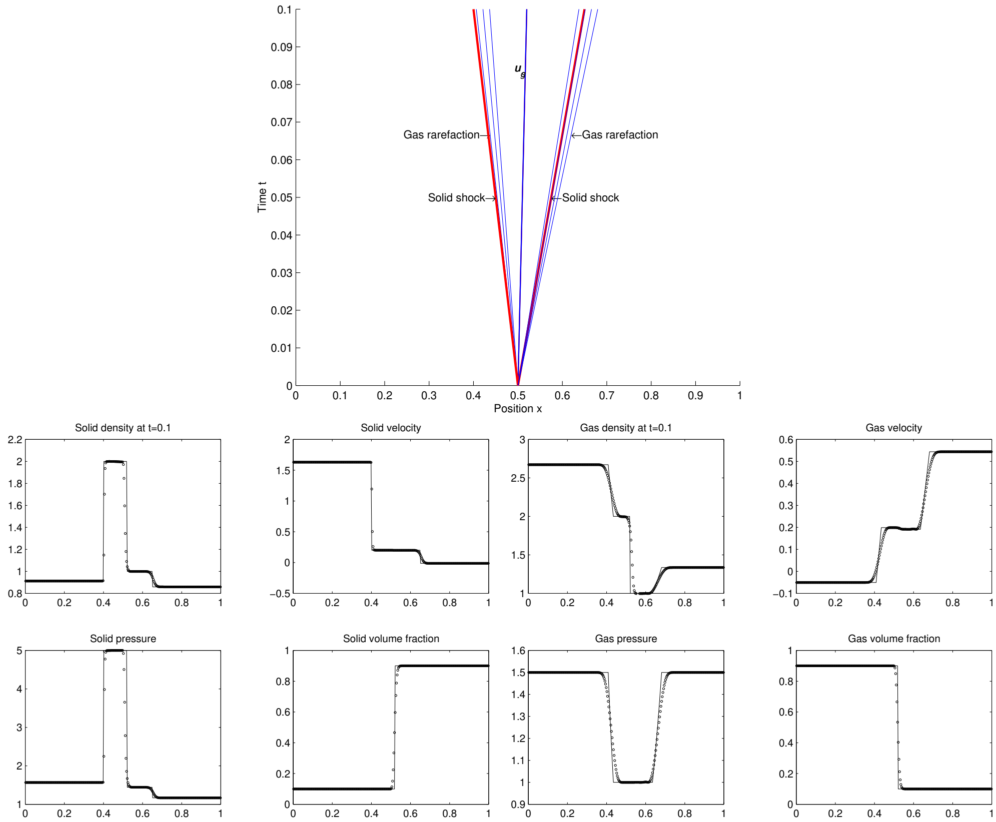

Figure 12: The Riemann problem for Test 3.

Test 4: Gas shock approaches solid contact In the limit, i.e. when the gas shock coincides with the solid contact, the jump conditions across this "double discontinuity" are given in Section 6. To achieve such a configuration, one may take the following initial data

Phase k	α_{kL}	ρ_{kL}	u_{kL}	p_{kL}	α_{kR}	ρ_{kR}	u_{kR}	p_{kR}
a	0.5	2.1917	-0.995	3.0	0.1	0.6333	-1.1421	2.5011
b	0.5	6.3311	-0.789	1	0.9	0.4141	-0.6741	0.0291

The structure of the Riemann problem and the numerical results for this case is presented in Fig. 13.

Test 5: Gas rarefaction attached to the solid contact Consider the following Riemann problem

Phase k	α_{kL}	ρ_{kL}	u_{kL}	p_{kL}	α_{kR}	ρ_{kR}	u_{kR}	p_{kR}
a	0.5	2	-1	2	0.1	1	-1	8.3994
b	0.5	0.2702	-3.4016	0.1	0.9	0.4666	-2.6667	0.2148

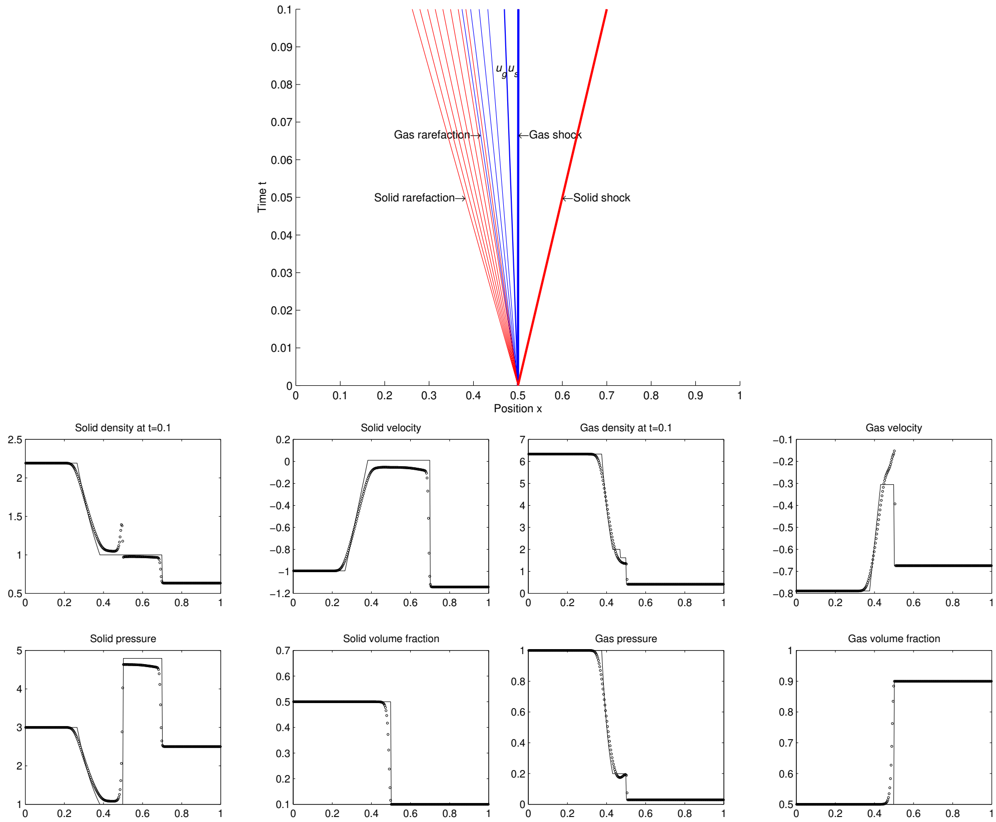

Figure 13: The Riemann problem for Test 4.

The exact solution to this test consists of a gas rarefaction, approachiung the solid contact from the left. In the limit, a parabolic degeneracy occurs, see Section 6. The structure of the Riemann problem and the numerical results are shown in Fig. 14.

8.3 Discussion of numerical results

The presented results have very a different quality for the various configurations. It is obvious that for big jumps in volume fraction the VFRoe method gives inadequate results. The numerical solution exhibits oscillations near the solid contact, which do not disappear as the mesh is refined. In the course of time, these oscillations are transported downstream, see e.g. the results for Test 1 in Fig. 10. The results for Test 2 in Fig. 11 show that the waves in different phases affect each other, which should not be the case. Observe the undershoots in solid density and velocity in Fig. 11. The methods behaves unsatisfactory in Test 4, where the gas shock approaches the solid contact. The numerical solution deviates strongly from the exact one, see Fig. 13. The discretization of the non-

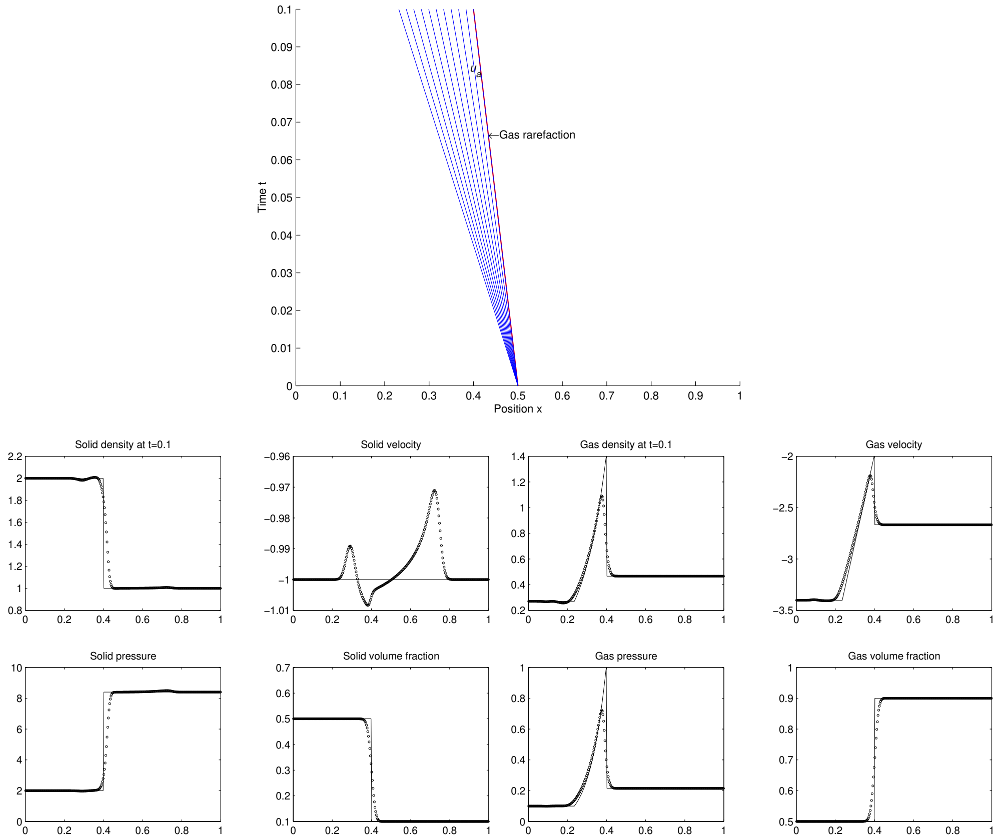

Figure 14: The Riemann problem for Test 5.

conservative terms (2.3) in VFRoe is obtained from the special case of constant velocity and pressure, see [1] for details. For Test 4, this is of course violated, and this is the reason for the wrong numerical solution in Fig. 13.

On the other hand, when the jump in volume fraction is not too big, the method is quite reliable, see e.g. the results for the Euler equations in the duct in Fig. 9. The results are also good for Test 3, see Fig. 12.

References

[1] N. Andrianov, R. Saurel, and G. Warnecke, A simple method for compressible multiphase mixtures and interfaces, accepted in *Int. J. Numer. Meth. Fluids*. Also available as INRIA preprint at `http://www.inria.fr/rrrt/rr-4247.html`.

[2] M.R. Baer, and J. W. Nunziato, A two-phase mixture theory for the deflagration-to-detonation transition (DDT) in reactive granular materials,

Int. J. of Multiphase Flows, **12**, 861-889 (1986).

[3] J. B. Bdzil, R. Menikoff, S. F. Son, A. K. Kapila, D. S. Stewart, Two-phase modeling of deflagration-to-detonation transition in granular materials: A critical examination of modeling issues, *Phys. Fluids* **11** (2), 378-402 (1999).

[4] R. Courant and K. O. Friedrichs, *Supersonic flow and shock waves,* Springer, New York, 1999.

[5] V. G. Dulov, Decay of an arbitrary initial discontinuity of the gas parameters across a jump-discontinuity in the cross-sectional area, *Vestnik Leningrad. Univ.* **19** (4), 76-99 (1958). (In Russian)

[6] P. Embid and M. Baer, Mathematical analysis of a two-phase continuum mixture theory, *Continuum Mech. Thermodyn.* **4**, 279-312 (1992).

[7] A. K. Kapila, S. F. Son, J. B. Bdzil, R. Menikoff, and D. S. Stewart, Two-phase modeling of DDT: structure of the velocity-relaxation zone, *Phys. Fluids* **9** (12), 3885-3897 (1997).

[8] A. K. Kapila, R. Menikoff, J. B. Bdzil, S. F. Son, and D. S. Stewart, Two-phase modeling of deflagration-to-detonation transition in granular materials: Reduced equations, *Phys. Fluids* **13** (10), 3002-3024 (2001).

[9] A. G. Kulikovskii, N. V. Pogorelov, and A. Yu. Semenov, *Mathematical aspects of numerical solution of hyperbolic systems,* CRC Press, Boca Raton, 2001.

[10] L. D. Landau and E. M. Lifschitz, *Fluid mechanics,* Pergamon Press, Oxford, 1987.

[11] V. H. Ransom, Numerical benchmark tests, in *Multiphase Science and Technology*, vol. 3, G. F. Hewitt, J. M. Delhaye, N. Zuber (eds). Hemisphere, Washington, 1987.

[12] R. Saurel and O. LeMetayer, A multiphase model for compressible flows with interfaces, shocks, detonation waves and cavitation, *J. Fluid Mech.* **431**, 239-271 (2001).

[13] J. Smoller, *Shock waves and reaction–diffusion equations,* Springer, New York, 1983.

[14] H. B. Stewart and B. Wendroff, Two-phase flow: models and methods, *J. Comput. Phys.* **56**, 363-409 (1984).

[15] E. F. Toro, *Riemann solvers and numerical methods for fluid dynamics*, Springer, Berlin, 1999.

[16] I. K. Yaushev, Decay of an arbitrary discontinuity in a channel with a jump in the cross-sectional area, *Izv. Sibirsk. Akad. Nauk SSSR* **8** (2), 109-120 (1967). (In Russian)

[17] M. J. Zucrow, J. D. Hoffman, *Gas dynamics,* vol. 2, John Wiley & Sons, 1977.